AD-A122 024 USE OF THE AURORA FLASH X-RAY MACHINE AS A SOURCE-REGION EMP SIMULATOR AN..(U) HARRY DIAMOND LABS ADELPHI MD G MERKEL ET AL. OCT 82 HDL-TR-1975 1/1

UNCLASSIFIED MIPR-80-581 F/G 20/14 NL

END

FILMED

DTIC

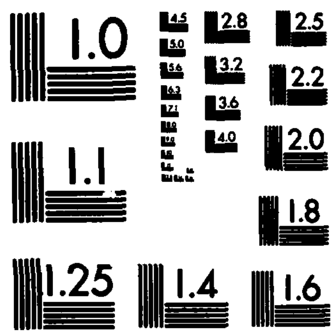

13

HDL-TR-1975
October 1982

Use of the AURORA Flash X-Ray Machine as a Source-Region EMP Simulator and Antenna Coupling Analysis Facility

by George Merkel
William D. Scharf
Daniel J. Spohn

U.S. Army Electronics Research and Development Command
Harry Diamond Laboratories
Adelphi, MD 20783

UNCLASSIFIED

SECURITY CLASSIFICATION OF THIS PAGE (When Data Entered)

REPORT DOCUMENTATION PAGE		READ INSTRUCTIONS BEFORE COMPLETING FORM
1. REPORT NUMBER HDL-TR-1975	2. GOVT ACCESSION NO. AD-B069428	3. RECIPIENT'S CATALOG NUMBER
4. TITLE (and Subtitle) Use of the AURORA Flash X-Ray Machine as a Source-Region EMP Simulator and Antenna Coupling Analysis Facility		5. TYPE OF REPORT & PERIOD COVERED Technical Report 6. PERFORMING ORG. REPORT NUMBER
7. AUTHOR(s) George Merkel William D. Scharf Daniel J. Spohn		8. CONTRACT OR GRANT NUMBER(s)
9. PERFORMING ORGANIZATION NAME AND ADDRESS Harry Diamond Laboratories 2800 Powder Mill Road Adelphi, MD 20783		10. PROGRAM ELEMENT, PROJECT, TASK AREA & WORK UNIT NUMBERS Program Ele.: 62704H
11. CONTROLLING OFFICE NAME AND ADDRESS Director Defense Nuclear Agency Washington, DC 20305		12. REPORT DATE October 1982 13. NUMBER OF PAGES
14. MONITORING AGENCY NAME & ADDRESS(if different from Controlling Office)		15. SECURITY CLASS. (of this report) UNCLASSIFIED 15a. DECLASSIFICATION/DOWNGRADING SCHEDULE

16. DISTRIBUTION STATEMENT (of this Report)

Approved for public release; distribution unlimited.

17. DISTRIBUTION STATEMENT (of the abstract entered in Block 20, if different from Report)

18. SUPPLEMENTARY NOTES

HDL Project: E050E3
PRON: WJ0--3101WJA9
MIPR-ORDER NO.: 80-581

19. KEY WORDS (Continue on reverse side if necessary and identify by block number)

Electromagnetic pulse
Antennas
Nuclear source-region simulation
AURORA

20. ABSTRACT (Continue on reverse side if necessary and identify by block number)

In the AURORA flash x-ray machine, a bremsstrahlung spectrum is produced in four thick tantalum targets by four synchronous 10-MeV electron beams. The bremsstrahlung then produces an electromagnetic pulse (EMP) signal through the same mechanism as does a nuclear bomb. It induces Compton electron currents in the AURORA test cell chamber (20 × 15 × 5 m). As the Compton electrons are slowed down, they ionize the air and also produce an electromagnetic field in the chamber. However, the Compton current is

20. Abstract (Cont'd)

confined to a relatively small volume so that a relatively small electromagnetic field is produced, rendering the unmodified AURORA machine unsuitable as a source-region EMP (SREMP) simulator.

A large parallel-plate transmission line has been designed to produce a "threat-like" EMP pulse. This transmission-line simulator can be placed in the AURORA test cell. When AURORA and the line are fired synchronously, an SREMP-like environment is produced, with AURORA providing the time-varying air conductivity.

The configuration described above has been used to study the behavior of antennas in a time-varying conductive medium. Experimental data are presented. Also presented are equivalent circuit models used in the analysis of the data. Circuit models for antennas are obtained using the "method of moments"--a frequency-domain technique. The circuit models describe the antenna's interaction with the environment (through the equivalent height circuit) and with the loading circuit (through the impedance circuit). The modification of these circuits to deal with time-varying air conductivity is discussed (this complicates a frequency-domain approach). Comparisons are made between data taken in the simulator and calculations made using the circuit models.

CONTENTS

FIGURES

Figures (Cont'd)

FIGURES (Cont'd)

Page

1. INTRODUCTION

Historically, low-altitude electromagnetic pulse (LAEMP) research has emphasized strategic interests. Both calculational techniques (considering only a localized environment) and testing (using environments generated during underground nuclear tests) have been widely applied to systems expected to survive extreme overpressures. Recently, the possibility of limited nuclear war on the tactical battlefield has been seriously discussed, and interest has heightened in estimating the response of tactical equipment--that which can be expected to survive a much less severe environment. Unfortunately, this region cannot be effectively simulated with underground detonations. Therefore, attention has been directed toward other methods of simulating this environment in a laboratory setting, as well as developing and verifying applicable calculational techniques.

This paper describes a technique for the simulation of the tactical source-region EMP (SREMP) environment and for antenna coupling analysis. This technique is being developed at the U.S. Army's Harry Diamond Laboratories (HDL). In many cases, only a cursory discussion is provided, with many of the technical details omitted. Those details will be published in a series of technical reports, many of which are presently being prepared.

2. TACTICAL ENVIRONMENT

It has been recognized that no tactical system can be expected to survive a direct nuclear attack, but tactical equipment can be expected to operate near nuclear detonations. A method has been developed by the U.S. Army's Nuclear and Chemical Agency, for setting attainable survivability criteria for such equipment.[1] The criteria are based on a "balanced hardening" philosophy which, simply stated, is that a system should be hardened against any particular nuclear effect only to a level commensurate with the system's hardness against all other effects. For tactical systems, this level is often dominated by the survivability of the system's operator to blast, thermal radiation, and initial radiation effects. Systems should be designed to survive the maximum EMP which could be experienced at a range (varying for different yield weapons) consistent with operator survivability. The environment is characterized not only by electromagnetic fields but also by the ionizing radiation. This ionizing radiation complicates the electromagnetic effects by introducing current sources and time-varying air conductivity.

[1]*Nuclear Survivability Criteria for Army Tactical Equipment (U), U.S. Army Nuclear Agency, NUA-C-5400-74 (August 1974). (CONFIDENTIAL-RESTRICTED DATA)*

3. AURORA FLASH X-RAY MACHINE

The Defense Nuclear Agency's AURORA Flash X-Ray Facility at HDL in Adelphi, MD,[2-4] is the largest of its type. This machine produces bremsstrahlung in four thick tantalum targets by four synchronous pulsed 8-MeV, 230-kA electron beams. At a total energy of about 1.2 MJ, the machine was designed to provide a high-dose gamma radiation environment over approximately a 1-m cube (shown later, sect. 4.1, fig. 4(a)). Fortunately, the facility is equipped with a large test cell (19.8 × 14.6 × 4.6 m), rendering it suitable for experiments requiring lower levels of radiation over a considerably larger volume. The radiation and resulting Compton currents, acting through the same physical mechanisms as expected from a nuclear detonation, produce an EMP environment in the facility's test chamber which is qualitatively similar to that resulting from a nuclear detonation. However, because of several factors, including the time history of the radiation, the geometry of the sources, the small volume of Compton current, and the conductive walls of the test chamber, the unmodified AURORA facility is unsuitable as a source-region simulator. Figure 1 shows a typical normalized gamma radiation pulse generated by AURORA. The resulting air conductivity waveform has approximately the same shape, with peaks varying from 10^{-1} mho/m at the "hot spot" to about 10^{-4} mho/m at the back of the test chamber. This gamma pulse time history differs from the prompt radiation which would produce the survivability criteria environment.

At a point in the chamber where the peak conductivity is approximately that associated with operator survivability (10 m from the source), the time histories of the conductivity and vertical electric fields differ significantly from those of the survivability criteria. Figure 2 shows the vertical electric field and conductivity at the point as predicted by AUR3D, a computer code produced by William Crevier of Mission Research Corporation to simulate the AURORA environment. These results compare favorably with experimental results obtained by HDL at the same location.[5] Neither the electric field nor the conductivity produced by AURORA model well the electric field and conductivity which are expected in a typical tactical EMP environment. They differ substantially in peak amplitude, risetime, and late-time behavior.

---

[2] *Hans Fleischmann, High Current Electron Beams, Physics Today, 28, 5 (May 1975), 34.*

[3] *Gerold Yonas, Fusion Power with Particle Beams, Scientific American, (November 1978), 50.*

[4] *B. Bernstein and I. Smith, AURORA, An Electron Accelerator, IEEE Trans Nucl Sci, NS-20, 3 (June 1973).*

[5] *L. M. Anderson et al, Status of AURORA Environment Calculations, IEEE Trans Nucl Sci, NS-25, 6 (December 1978).*

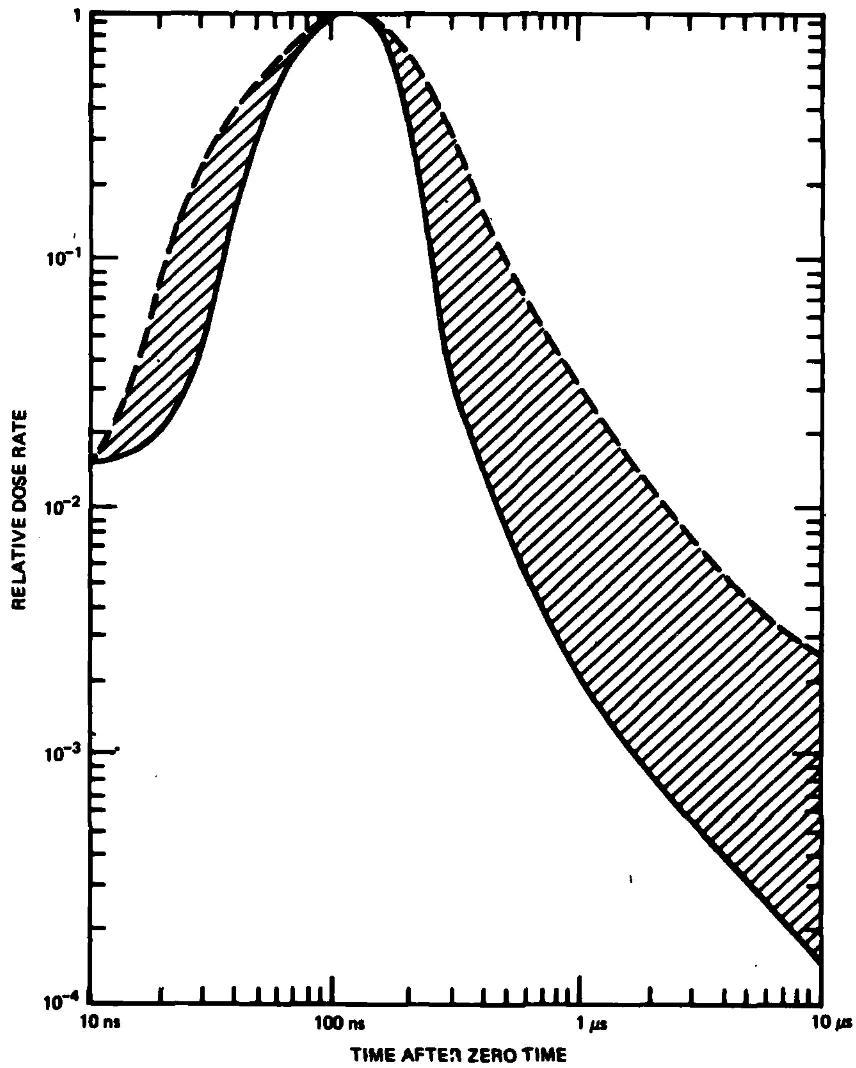

Figure 1. AURORA gamma pulse. A typical pulse can be expected to fall within the shaded area.

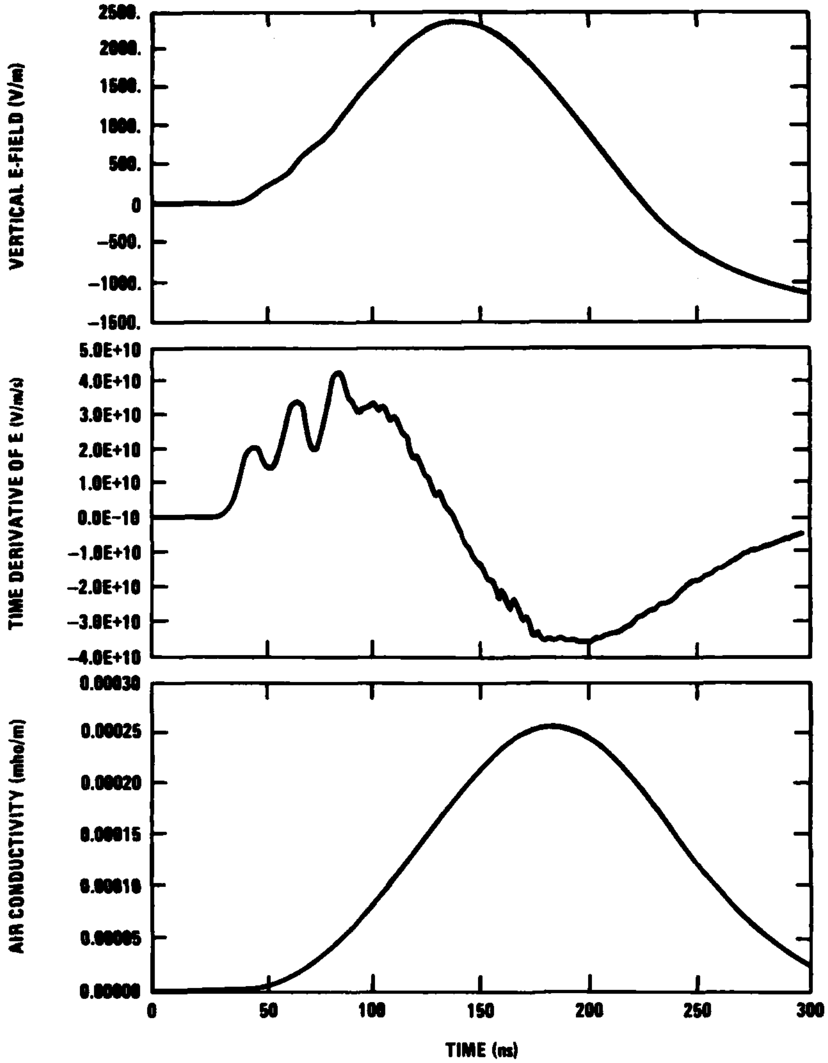

Figure 2. E-field, its time derivative, and air conductivity at base of antenna at 10 m as calculated by AUR3D with no antenna present.

Consideration of a short monopole antenna demonstrates the inadequacy of the AURORA environment.[6] The short-circuit current in a short antenna is given as

$$I_s = \frac{1}{2} hC \left(\frac{dE}{dt} + \frac{\sigma E}{\varepsilon_o} \right) ,$$

where

h = the height of the antenna
C = the capacitance of the antenna = $\frac{h}{cZ_o}$
$Z_o = 60\left[2\ln\left(\frac{2h}{a}\right) - 3.39\right]$
a = the antenna wire radius
E = the incident electric field
σ = the conductivity of the medium
ε_o = the permittivity of the medium
c = velocity of light

Figure 3 shows the response of the short monopole antenna exposed to the AURORA environment at a point where the peak conductivity is consistent with survivability criteria. The good agreement between AURORA data and this model, which does not include any resonant behavior, suggests that the unmodified AURORA is unsuitable as an SREMP simulator. In a typical tactical environment, resonances would be excited on a 1-m monopole antenna such as the one used in gathering these data.

4. MODIFICATION OF AURORA ENVIRONMENT

4.1 First-Order Modification

It is apparent from the foregoing discussion that E-fields, which are larger and have shorter risetimes than those available from unmodified AURORA, are essential for even the most rudimentary simulation. However, AURORA is the only available facility which can provide acceptable time-varying conductivity levels over a large enough volume to be useful. It appears that, in order to take advantage of this unique feature of AURORA, one should make use of a supplementary EMP source. For the work reported here, this supplementary source took the form of a large (12 × 3 × 5 m) parallel-plate transmission line--designed with the assistance of William Crevier. The two plates of this line were mounted vertically in the test chamber with a separation of

[6] *R. Manriquez, G. Merkel, W. D. Scharf, and D. Spohn, Electrically Short Monopole Antenna Response in an Ionized Air Environment--Determination of Ionized Air Conductivity, IEEE Trans Nucl Sci,* 26*, 6 (December 1979).*

3 m and stretched laterally across the chamber from one side wall to the other. (See fig. 4(a) to (c).) The hindmost plate (furthest from the "hot spot") is grounded to the test cell floor and ceiling, but the front plate is isolated from ground and is driven by a 100-kV pulser. The distance between the hot plate and both the floor and ceiling is about 1 m, and the plate curves in at both the top and bottom, so that the plate separation at top and bottom is only about 230 cm. This curvature focuses the field lines so that a relatively uniform E-field is achieved at half-height, where experimental apparatus is mounted. In an attempt to minimize impedance mismatches, both the ground plate and the hot plate were tapered out from the drive point. The line tapers out from a separation of 10 cm at the drive point to the full 3-m separation over a distance of 4 m. The line was terminated at the other end in an anechoic resistive curtain connecting the two plates and in two resistive bundles connecting the hot plate to the floor and ceiling. The termination was designed to distribute the current roughly along field lines. The entire transmission line was constructed as a unit on a sturdy wooden frame, so that it could be moved back and forth in the test cell--providing a means of adjusting the conductivity level. The line was driven at the drive point, through 50 ft of 50-ohm cable, from a 100-kV pulser built by Pulsar, Inc., which delivers a pulse with a risetime of about 20 ns and a decay time of about 2 μs. Thus, a peak field of about 33 kV/m is seen in the line.

It should be noted that the E-field signal is by no means independent of the AURORA-induced air conductivity. In order to analyze the effect of ionizing radiation on the transmission line, we must know the air conductivity as a function of ionizing radiation. In 1977, HDL carried out a number of "pie-pan" experiments[7] to measure air conductivities for a range of humidities. This work, analyzed by Dean May,[8] is summarized in figure 5.

As an aid to visualizing the effect of the conductivity, consider the simple circuit model of figure 6. (This is intended only as a very rough qualitative description of the interaction.) In this model, the pulse (which has a long discharge time ≈ 2 μs) is assumed to be a perfect voltage source. The 50-ohm cable is modelled as an inductor, the line as a capacitor, and the termination as a resistor. (Of course, in reality, both the line and the cable have distributed inductance and distributed capacitance.)

---

[7] *W. F. Crevier, C. L. Longmire, G. Merkel, D. J. Spohn, Air Chemistry and Boundary Layer Studies with AURORA, IEEE Trans Nucl Sci, NS-24, 6 (December 1977).*

[8] *Dean L. May, Electron Mobility and Electron Attachment Rate in an Electromagnetic Pulse Air Environment, Harry Diamond Laboratories Student Technical Symposium (17 to 18 August 1977), 87.*

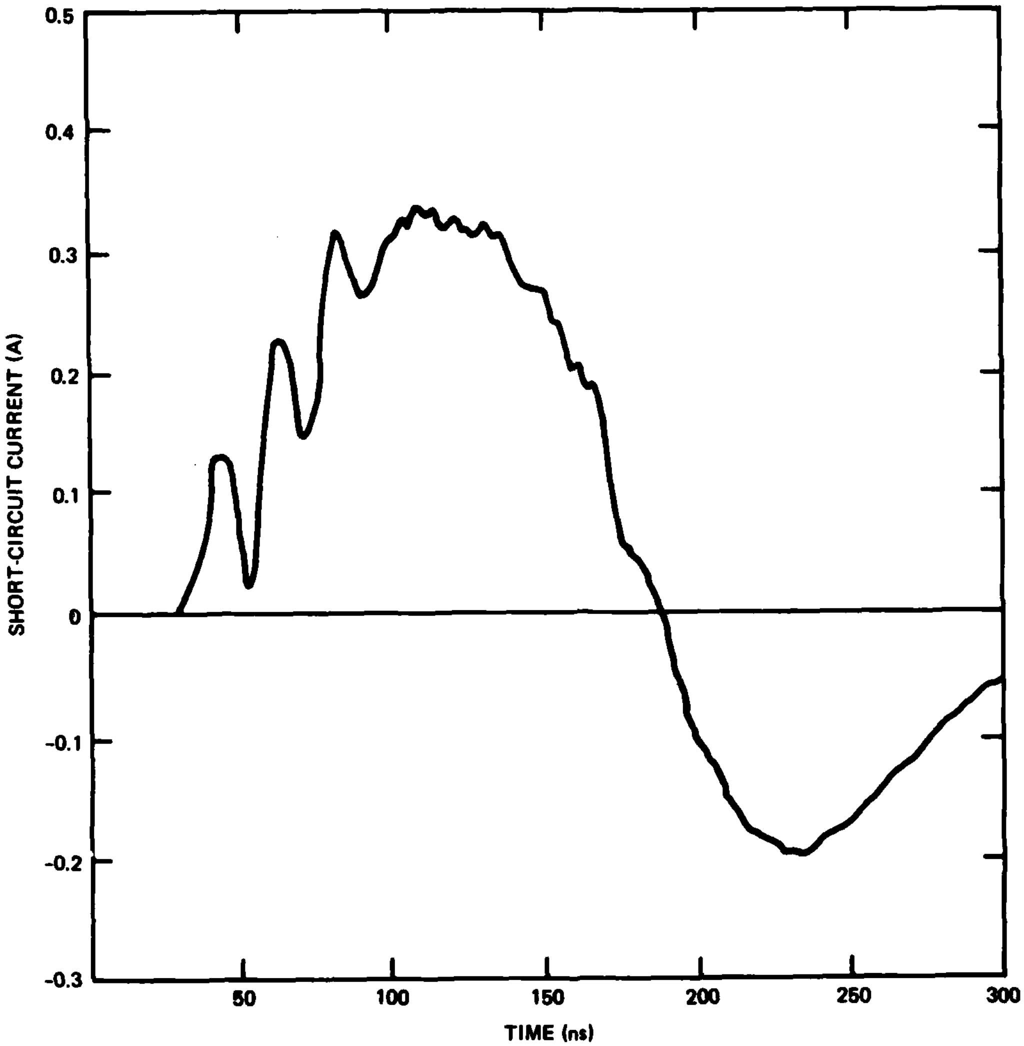

Figure 3. Short-circuit current on 1-m monopole antenna 10 m from AURORA source.

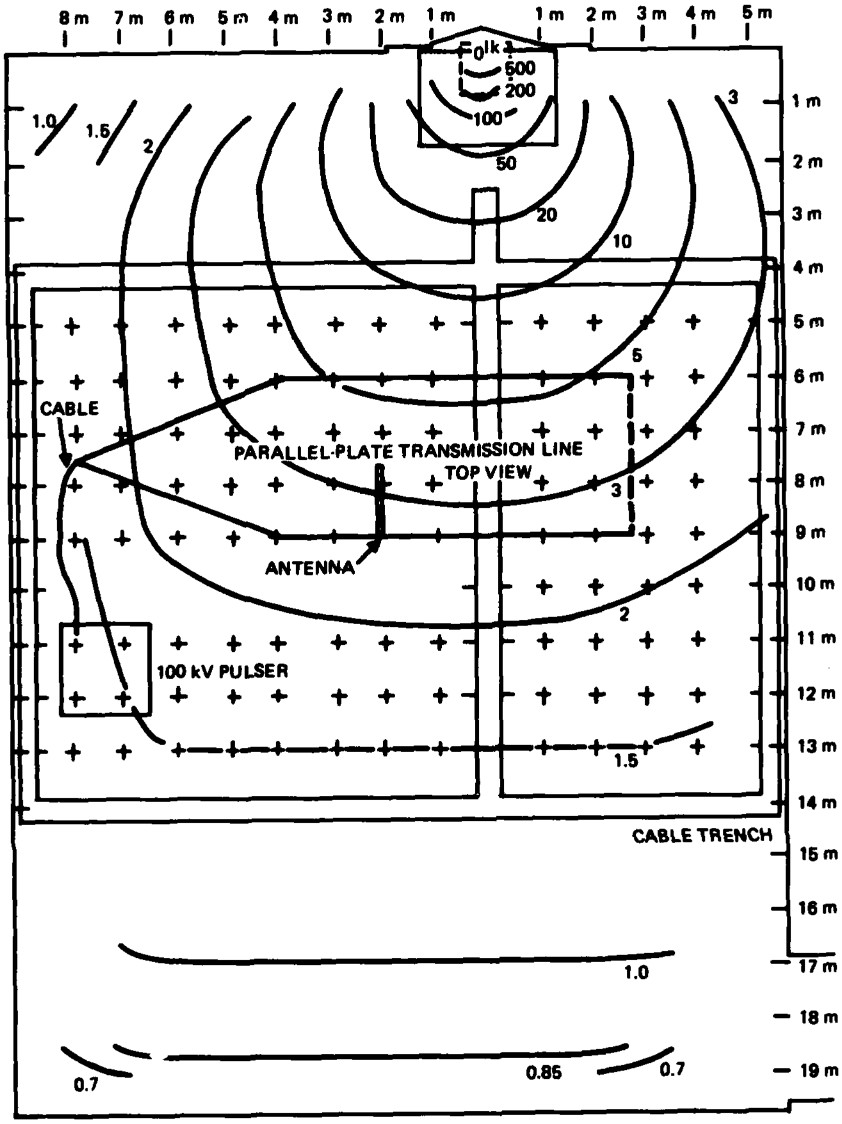

Figure 4. Views of transmission line in AURORA test cell: (a) isodose contours and schematic view of auxiliary parallel-plate transmission line in AURORA test cell.

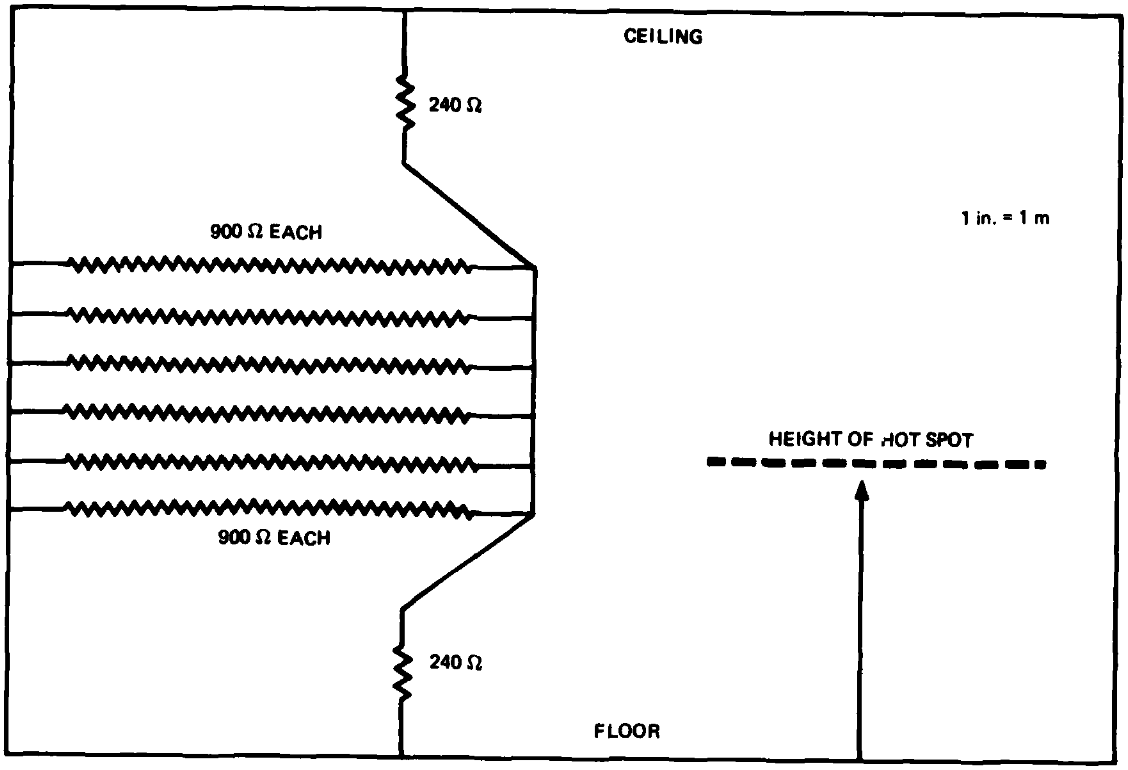

Figure 4 (cont'd). Views of transmission line in AURORA test cell: (b) Side view of transmission line.

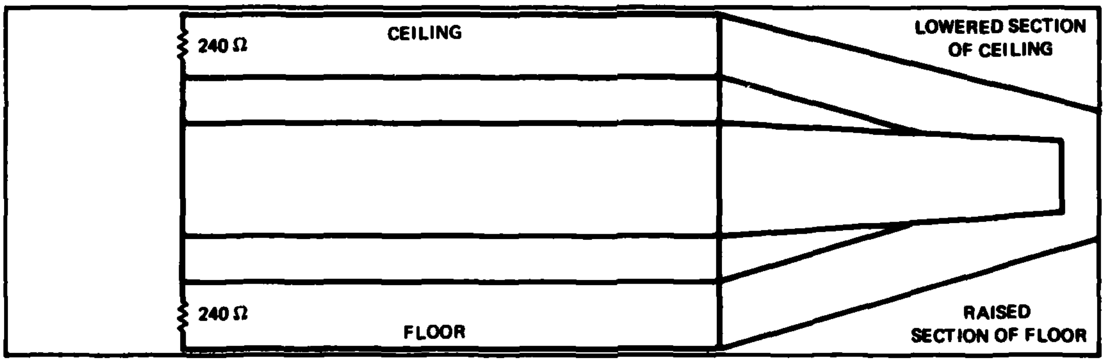

Figure 4 (cont'd). View of transmission line in AURORA test cell: (c) from front wall of AURORA.

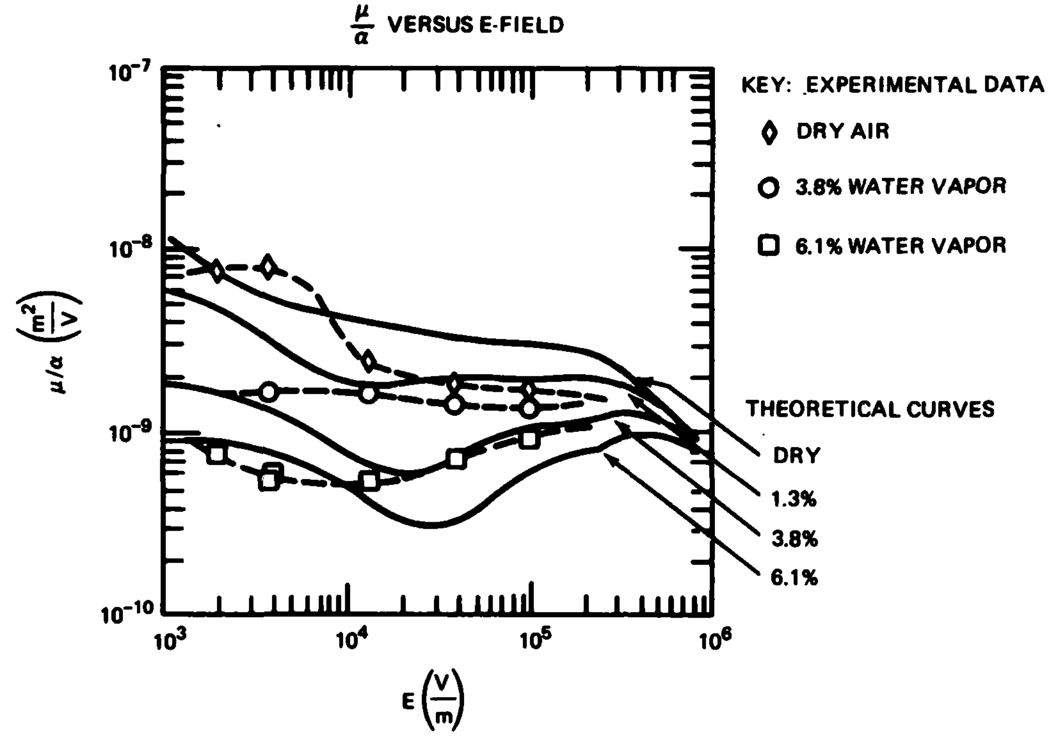

Figure 5. Theoretical and experimental ratios of electron mobility to electron attachment rate versus E-field for dry and moist air. To a very good approximation, air conductivity is given by $\sigma(E) = \dot{\gamma}q\mu(E)/\alpha(E)$, where $\dot{\gamma}$ is the ionization rate in ion pairs per second. The 3.8-percent water vapor curve is nearly flat; i.e., conductivity at 3.8-percent water vapor is independent of electric field. Therefore, to a very good approximation, at 3.8-percent water vapor, air conductivity, $\sigma(t)$, is given by $\sigma(t) = 0.5 \times 10^{-12}\ F\gamma(t)$, where $F\gamma$ is in roentgens per second. Theoretical curves are calculated in the manner described in Air Chemistry and Boundary Layer Studies with AURORA, by Crevier, Longmire, Merkel, and Spohn, IEEE Trans. Nucl. Sci., NS-24 (December 1977).

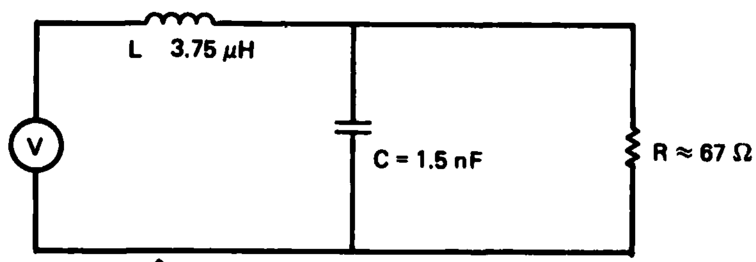

Figure 6. Simplified equivalent circuit of transmission-line simulator.

If the capacitor dielectric (air) is subjected to pulsed ionizing radiation causing a peak conductivity of 10^{-3} mho/m, the capacitor "turns into" a 6-ohm resistor. When the conductivity disappears (when the radiation stops), it turns back into a capacitor.

$$G_{peak} = C\,\frac{\sigma}{\varepsilon} = \left(1.5 \times 10^{-9}\ \mathrm{F}\right)\left(\frac{10^{-3}\ \mathrm{mho/m}}{9 \times 10^{-12}\ \frac{\mathrm{F}}{\mathrm{m}}}\right) = \frac{1}{6}\ \mathrm{mho}.$$

The circuit appearing in figure 7 can therefore be described even more simply by the following equation:

$$V = L\,\frac{dI}{dt} + RI \quad .$$

This equation, in which V and R are functions of time, can be solved using the method of variation of parameters:

$$I(t) = e^{-\int_0^t r(t)dt} \int_0^t V(t)\, e^{\int_0^t t(t)dt}\, dt \quad ,$$

where

$$r(t) = \frac{R(t)}{L}, \text{ and } v(t) = \frac{V(t)}{L} \quad .$$

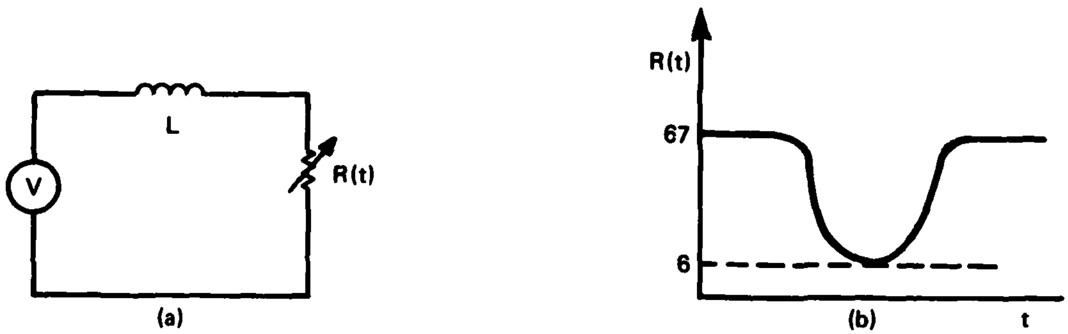

Figure 7. Extremely simplified equivalent circuit of transmission-line simulator.

Qualitatively, the reaction of the circuit to a pulsed dip in load resistance, with V constant, can be described as follows. As the resistance falls, a magnetic field (and hence a voltage drop) builds up in the inductor. The result is a drop in the voltage across the load. After the current reaches its peak, the energy stored in the magnetic field discharges back into the circuit, the current rises, and, if the load resistance has risen back to its full value in a time small compared to the discharge time of the inductor ($L/\bar{R}$, where $\bar{R}$ is an effective "average" value of the resistance), the voltage across the load will overshoot its quiescent level. This "inductive kick"[9,10] can be seen in both the measured and the calculated transmission-line voltage.

4.2 Suggested Further Modifications

The above description applies to the case of a constant voltage source. If there is appreciable conductivity during the risetime of the pulse, the desired pulse characteristics can be seriously degraded. At the criterion level of 3×10^{-4} mho/m peak conductivity, this degradation begins to be a problem. Figure 8 compares the E-field measured in the transmission line when the AURORA is fired to the E-field when the AURORA is not fired. Figure 9 is a similar comparison, but with the line 3 m closer to the AURORA hot spot. At this spot, the conductivity is much higher and there is a correspondingly greater E-field distortion. (Note that the relative firing times of AURORA and the pulser differ in the two figures. AURORA fired first in fig. 8, while the pulser fired first in fig. 9.) Since measurements are desired in an environment characterized both by conductivity and fast-rising fields, steps must be taken to minimize this waveform degradation. There are a number of approaches to the problem of reducing the inductive kick. The most obvious method is to position the line so that the conductivity is low. This clearly limits the utility of the transmission-line approach, since time-varying conductivity is an integral part of the environment to be simulated.

The inductive kick can also be limited by reducing the source impedance of the pulser (e.g., raising the capacitance) and shortening the 50-ohm feeder cable (lowering its inductance). However, one is limited ultimately by the distributed inductance of the transmission line itself. This can be handled by introducing a "slave line," which shares the same hot plate, but which is filled with a nonionizing gas

[9] *R. Manriquez, G. Merkel, and D. Spohn, Modification of the AURORA Environment, Harry Diamond Laboratories, HDL-PR-79-5 (October 1979).*

[10] *R. Manriquez, G. Merkel, and D. Spohn, Modification of the AURORA Electromagnetic Environment, IEEE Annual Conference on Nuclear and Space Radiation Effects (July 1978).*

such as SF_6 or CO_2. Physically, this can be achieved by erecting another ground plate in front of the hot plate and filling it with the appropriate gas (see fig. 10). The resulting line can then be visualized as a "coaxial cable" filled with nonionizing gas, except for an "experimentation sector," which is filled with ionizing gas (such as air or even N_2 for higher conductivity. See fig 11.) Of course, this "master-slave line" (or "sectored coax") will have a much lower impedance than the simple vertical-plate line. Thus, it will "waste" energy and make more demands on the pulser. The pulser impedance becomes a critical consideration. HDL has a variable voltage (40 to 400 kV) pulser with a decay time of 1.5 μs into 10 ohms. This pulser should be suitable for use with the sectored line.

It should also be mentioned that the ionization enhancement techniques outlined above may have implications for the study and simulation of the SREMP environment in the strategic case--for example, the MX System or the Ballistic Missile Defense System. Ordinarily, such systems (or their subsystems) could be tested only in an underground test. With our proposed methods, a much more cost-effective and repeatable series of tests could be conducted, which would reliably simulate at least the purely electromagnetic effects on such strategic systems.

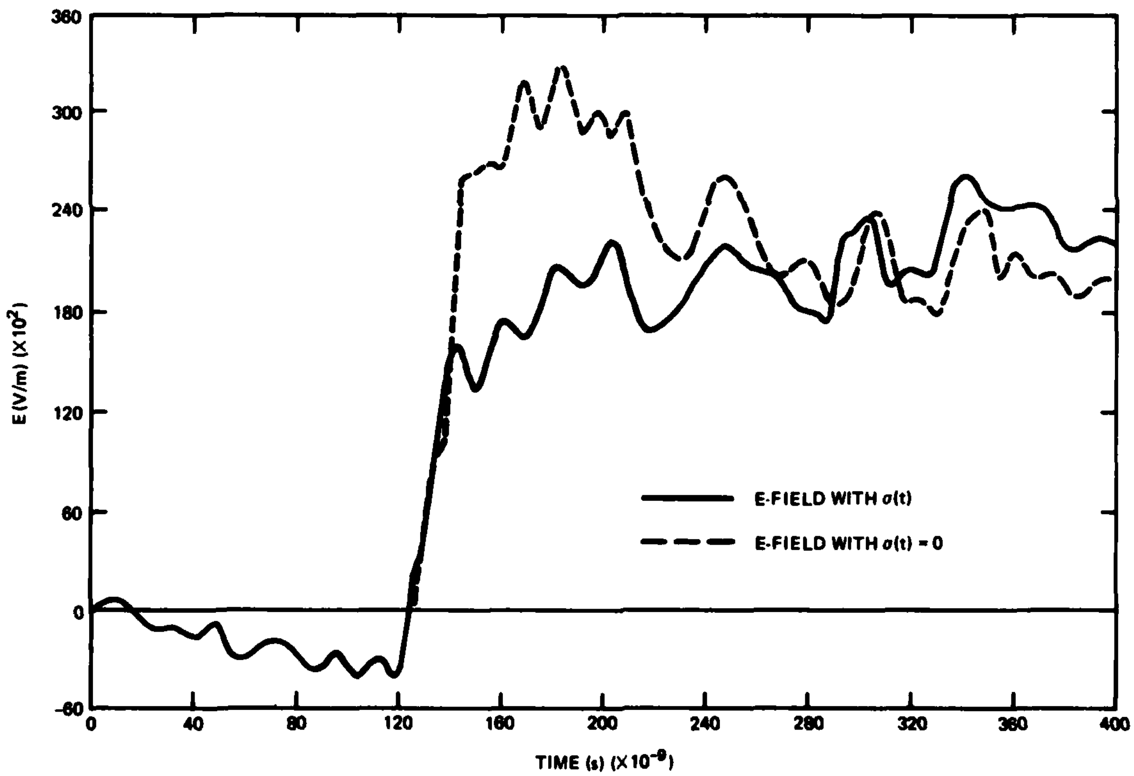

Figure 8. Comparison of E-field with and without ambient time-varying ionized air conductivity.

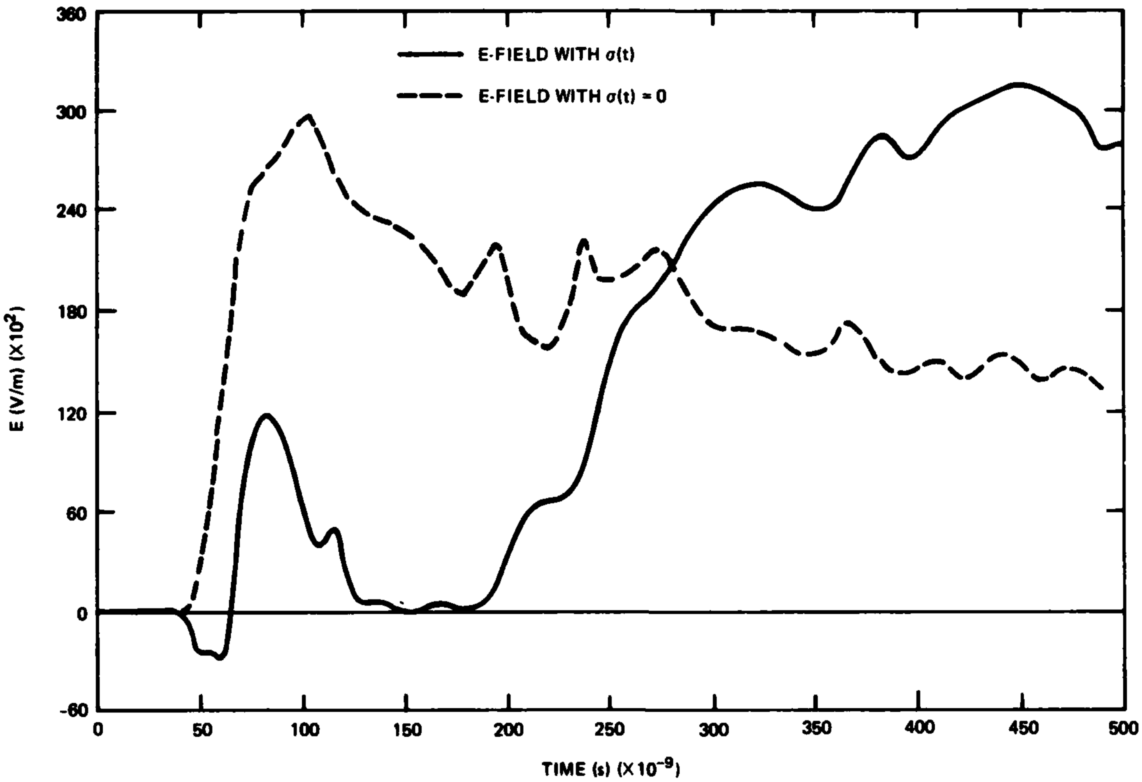

Figure 9. Comparison of E-field with and without ambient time-varying ionized air conductivity (3 m closer to hot spot than in figure 8.)

In the application of the scheme described above to strategic source-region simulation, there will be, for very high air conductivity, a self-shielding effect which will inhibit the propagation of the transmission-line mode. This effect becomes critical when the diffusion length over the time of interst is of the same order of magnitude as the transmission-line dimensions. Then, if the time of interest is 100 ns and a typical distance is 5 m,

$$L_{diff} \simeq \sqrt{\frac{4t}{\mu\sigma}} \simeq 5 \text{ m}$$

$$\sigma_{crit} \simeq \frac{4t}{\mu L^2_{diff}} = 0.013 \text{ mho/m} \quad .$$

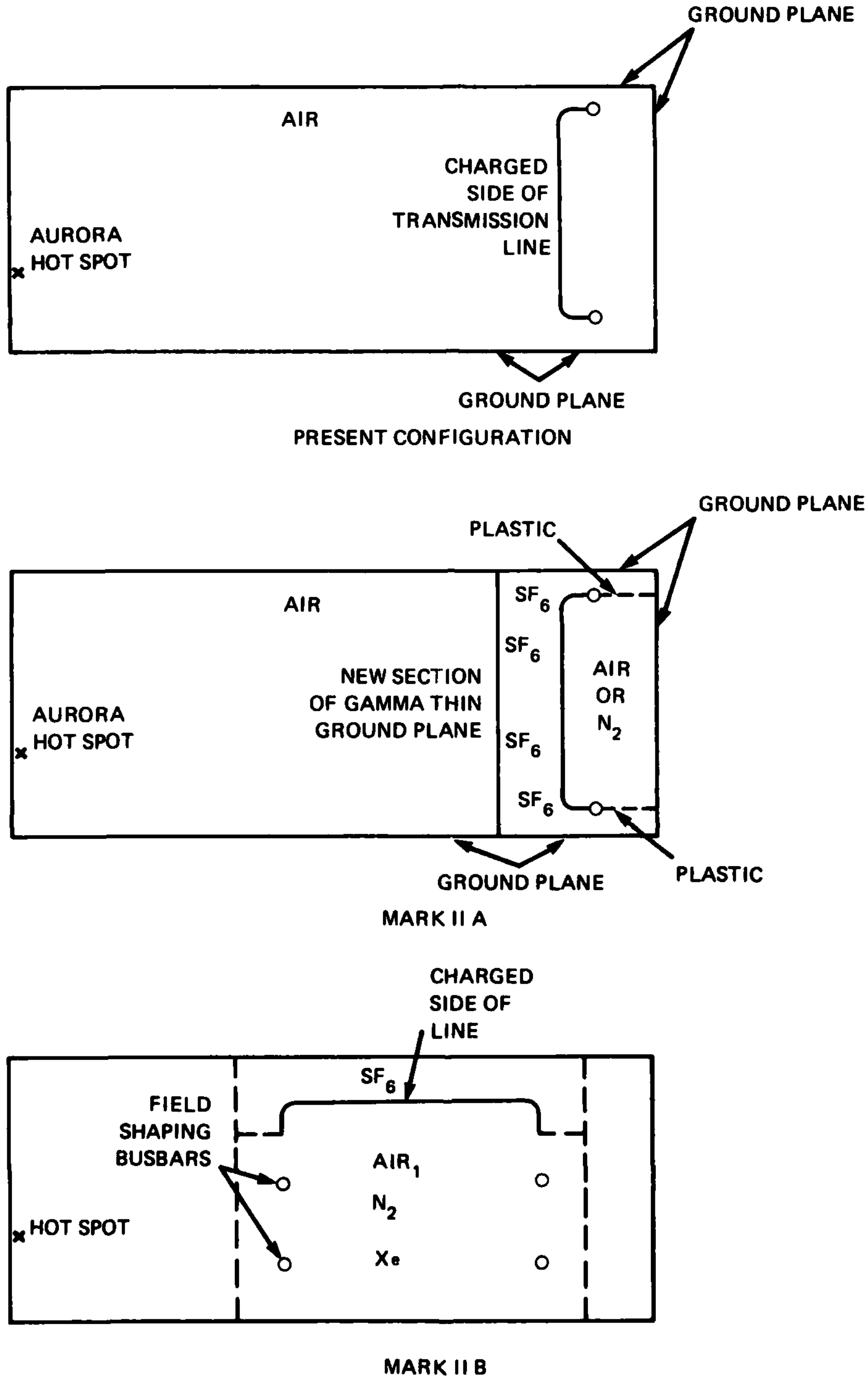

Figure 10. Comparison of present and proposed new improved transmission lines that would not suffer the "inductive kick."

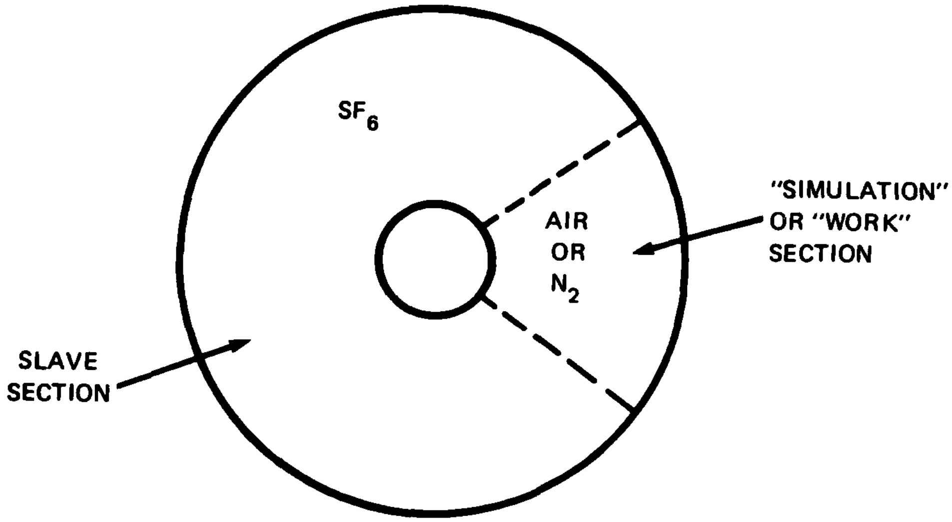

Figure 11. Generalization and simplification of slave line concept. The smaller the "work" section, the less the "inductive kick."

Thus, as long as the conductivity remains below about 0.01 mho/m, the transmission line should operate as described. For higher conductivity, the fields are determined (as they are in true nuclear EMP) by the local Compton current--i.e., the current within a diffusion sphere. As time progresses, this sphere $\left(|R - R_o| < L_{diff}\right)$ expands for two reasons: (1) the explicit square-root dependence of L_{diff} on t and (2) the implicit dependence through $\sigma(t)$, which decreases at late time.

For high conductivity levels, where the line self-shields, the most promising method of simulation seems to be the direct injection of high-energy electrons into the test volume. For instance, AURORA could be operated in the electron-beam mode, which is, in any case, a far more efficient use of the pulsed energy than is achieved in the more conventional bremsstrahlung mode. Electron irradiation of a large volume can be achieved through the use of a high-Z thin-target multiple-scattering "spray nozzle."

It should be noted that the proposed use of nonattaching gases will increase the fidelity of the $\sigma(t)$ waveform in two ways: (1) by causing a levelling-off arising from the constant resupply, through Compton creation and slowing down, of conduction electrons and (2) by enhancing the rise rate of the conductivity waveform. The free electron density n(t) obeys the equation

$$\frac{\partial n}{\partial t} = Q + \alpha n \quad ,$$

where Q is the ion-pair creation rate, and α is the attachment rate. (More generally, other recombination terms may be included.) The exact solution, with initial condition n(0) = 0, is

$$n(t) = \exp[-\alpha t] \int_0^t \exp[\alpha t] Q(\tau) d\tau \quad .$$

Note that, although the risetime is longer for low attachment rates, the rise rate is greater, leading to a greater contribution from the parametric-drive $\left(\frac{d\sigma}{dt} E\right)$ term. For xenon, the $\alpha = 0$ curve applies, and thus has the same shape as that for nitrogen, but the magnitude is enhanced by a factor of 5.5, due to higher Z (electron density) and due to a smaller electron energy loss per ion pair (36.3 eV for N_2, 21.4 eV for Xe).

In choosing gases for use in SREMP simulation, one must consider carefully their behavior when ionized. One important effect is the formation of boundary layers. In a low-density plasma, the well-known Debye sheath effect occurs at a metallic surface. In a plasma at atmospheric pressure (collision-dominated), the layer formation is dominated by a number of medium-dependent parameters--e.g., plasma frequency, collision frequency, ionic and electronic recombination and attachment rates,[11] ionic and electronic mobilities,[12] avalanching properties, etc. Electrode geometry is also very important. Small radii of curvature intensify fields and thus intensify both boundary-layer formation (through electron depletion) and avalanching. These two effects oppose each other so that, for instance, in nitrogen gas, the use of grid electrodes actually reduces the boundary-layer effects, as compared to the use of plate electrodes. These phenomena, whose descriptions here have been a bit oversimplified, are currently under study at HDL, and will be reported on soon.* Figure 12(a) compares the current through ionized air and through nitrogen around grid and plate electrodes in a large biased capacitor exposed to ionizing radiation. Figure 12(b) shows the apparatus used to obtain the data given in figure 12(a).

---

[11]*H. J. Longley and C. L. Longmire, Electron Mobility and Attachment Rate in Moist Air, Mission Research Corporation, MRC-N-222 (1975).*

[12]*C. E. Baum, The Calculation of Conduction Electron Parameters in Ionized Air, Electromagnetic Pulse Theoretical Notes, I, Note 6 (May 1967).*

**M. Bushell, C. Kenyon, G. Merkel, and W. D. Scharf, Electron Depletion Effects in the Nuclear EMP Source Region. To be submitted to IEEE Trans Nucl Sci.*

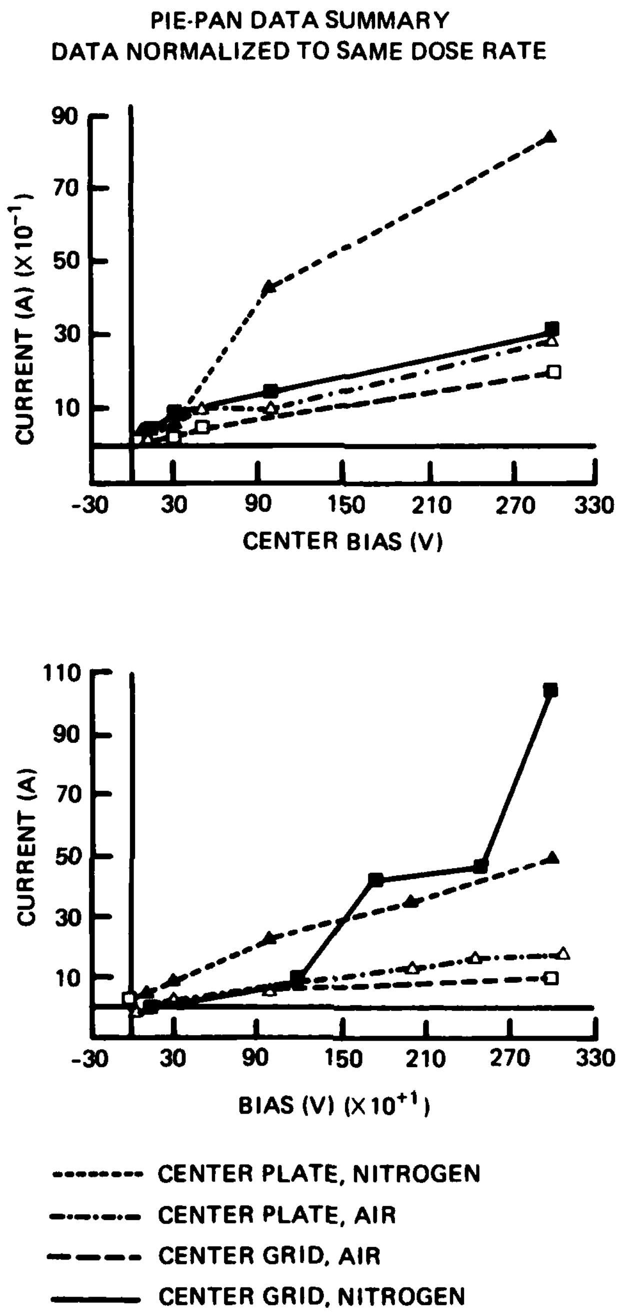

Figure 12. Influence of grid structure on "pie-pan" conductivity measurements: (a) Peak current as a function of bias voltage in air and nitrogen.

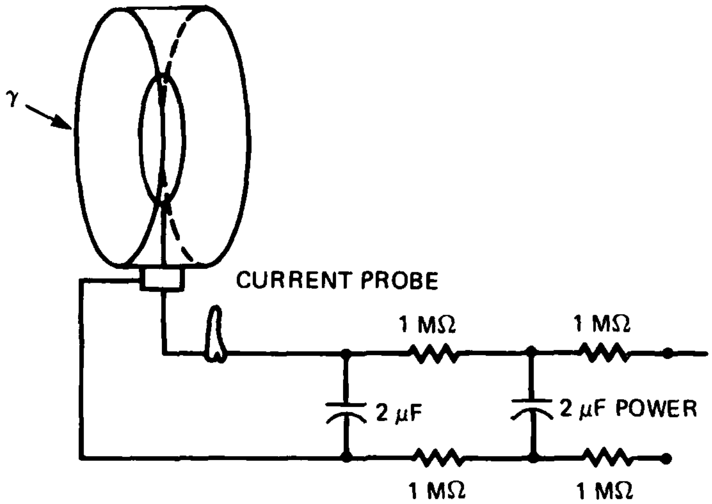

PIE-PAN SENSOR

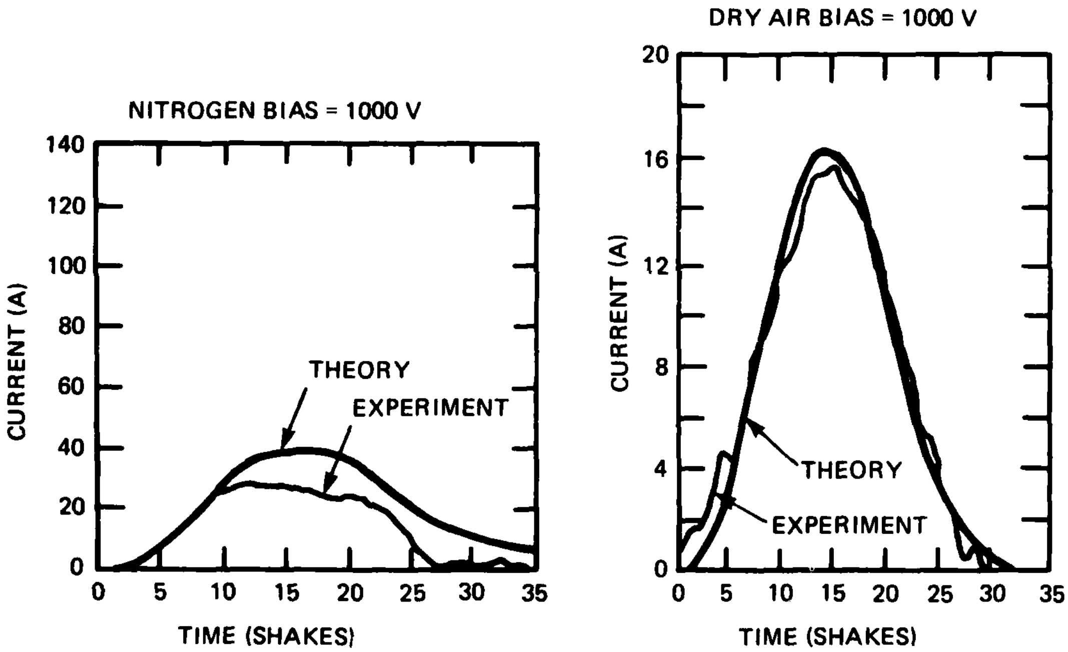

COMPARISON OF RESULTS

Figure 12 (cont'd). Influence of grid structure on "pie-pan" conductivity measurements: (b) Experimental setup used to obtain data shown in figure 12(a). Data marked "center grid" in figure 12(a) were obtained with grid in "pie-pan" rather than plate. Large value of nitrogen data with grid in center of "pie-pan" results from avalanching breakdown within the electron depletion boundary layer.

5. THEORETICAL INTERPRETATION OF INTERACTION OF TRANSMISSION-LINE AND IONIZING RADIATION

The detailed behavior of the transmission line when the AURORA is fired has been interpreted with a 36-section lumped-parameter transmission-line model.[13] The first 18 sections have been used to model the 50-ft 50-ohm coaxial cable, and the 12-m-long parallel plate has been modelled with a corresponding 18-section lumped-parameter network (LPN) transmission line. The best preliminary fit to the measured data was obtained when the parallel-plate line was assumed to be about 65 ohms. The line was terminated with a 67-ohm resistive screen. Figure 13 is a schematic diagram of the parallel-plate LPN model; figure 14 compares

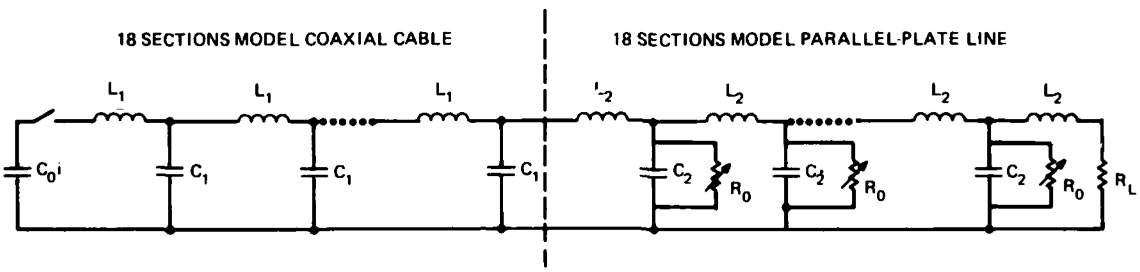

C_0 = PULSER CAPACITOR = 0.06 μF

$$\frac{1}{\sqrt{C_1L_1}} = \frac{\ell 1}{3\times|10|^{-8}}\sqrt{\epsilon} \qquad \sqrt{\frac{L_1}{C_1}} = 50\ \Omega = \text{IMPEDANCE OF COAXIAL CABLE}$$

$$\text{WHERE } \ell 1 = \frac{\text{LENGTH OF COAXIAL CABLE}}{\text{(NO. SECTIONS USED TO MODEL COAXIAL CABLE)}}$$

$$\frac{1}{\sqrt{C_2L_2}} = \frac{\ell 2}{3\times 10^{-8}} \qquad \sqrt{\frac{L_2}{C_2}} = 65\ \Omega = \text{IMPEDANCE OF PARALLEL-PLATE LINE}$$

$$\text{WHERE } \ell 2 = \frac{\text{LENGTH OF PARALLEL-PLATE TRANSMISSION LINE}}{\text{(NO. SECTIONS TO MODEL PARALLEL-PLATE LINE)}}$$

$R_L = 67\ \Omega$ = RESISTANCE OF TERMINATOR

Figure 13. Schematic of transmission-line lumped parameter network model.

---

[13] *M. Bushell, R. Manriquez, G. Merkel, W. Scharf, and D. Spohn, Source-Region EMP Simulator--A Parallel Plate Transmission Line in the AURORA Test Cell, IEEE Trans Nucl Sci, NS-27, 6 (December 1980).*

the E-field measured inside the parallel-plate transmission line and the value calculated with our LPN model when no conductivity is present.

A time-domain reflectometry (TDR) analysis of the transmission line indicates that the transition region between the coaxial cable and the parallel-plate line (the tapered section) has a varying impedance. In a forthcoming analysis, we will attempt to incorporate this information into our analysis, and we hope to reproduce the "fine structure" of the measured data.

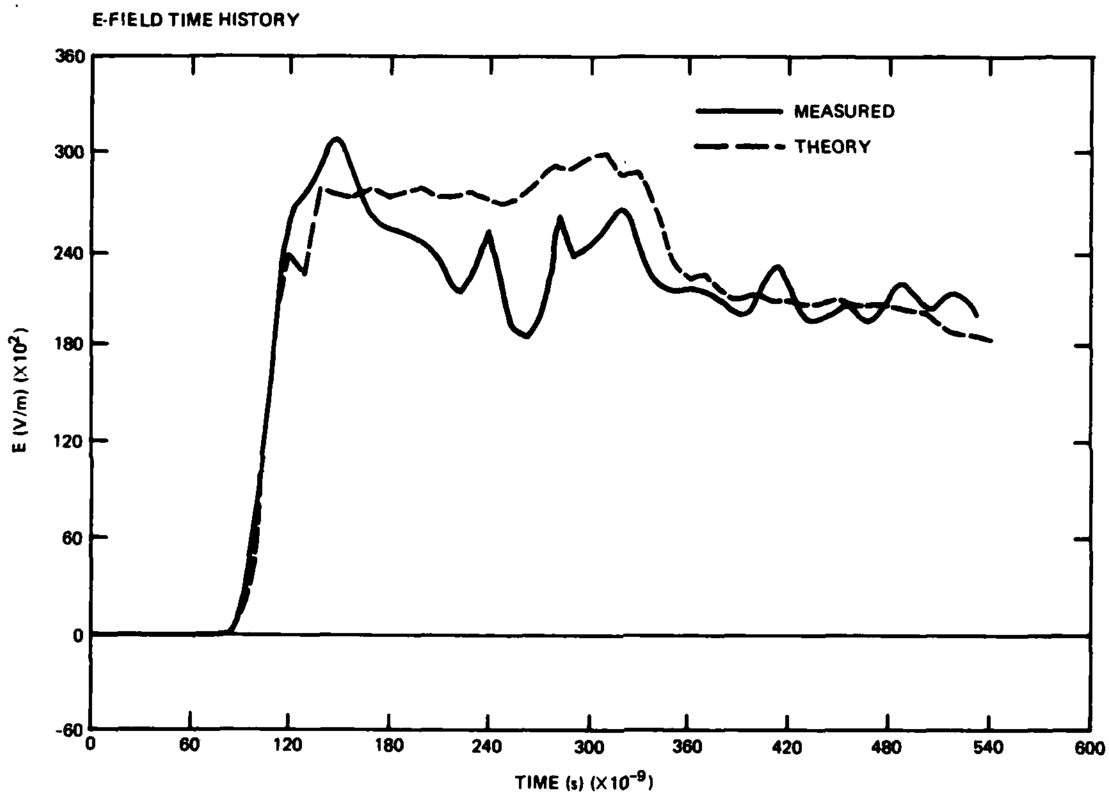

Figure 14. E-field inside parallel-plate transmission line (no conductivity).

The effect of ionizing radiation on the parallel-plate line is incorporated into the line model by introducing a time-varying resistor across each capacitor. The relationship between the value of this resistance and the ambient conductivity, $\sigma(t)$, is given by

$$R(t) = \frac{\varepsilon_o}{C\ \sigma(t)} .$$

This equation is a direct consequence of the fact that the value of the capacitance and the value of the resistance obtained by filling the capacitor with a conductance are both obtained by solving Laplace's equation.

Figures 15 to 20 compare an experimental E-field measurement and results calculated from the LPN model. The same experimental curve appears on all six figures. The theoretical curve of figure 15 uses a conductivity time history obtained with radiation dosimetry measurements and with the air chemistry parameters given by Dean May's analysis. Figures 16 to 20 give theoretical results using renormalizations of the same $\sigma(t)$ curve, each lower than the previous one by a factor of two.

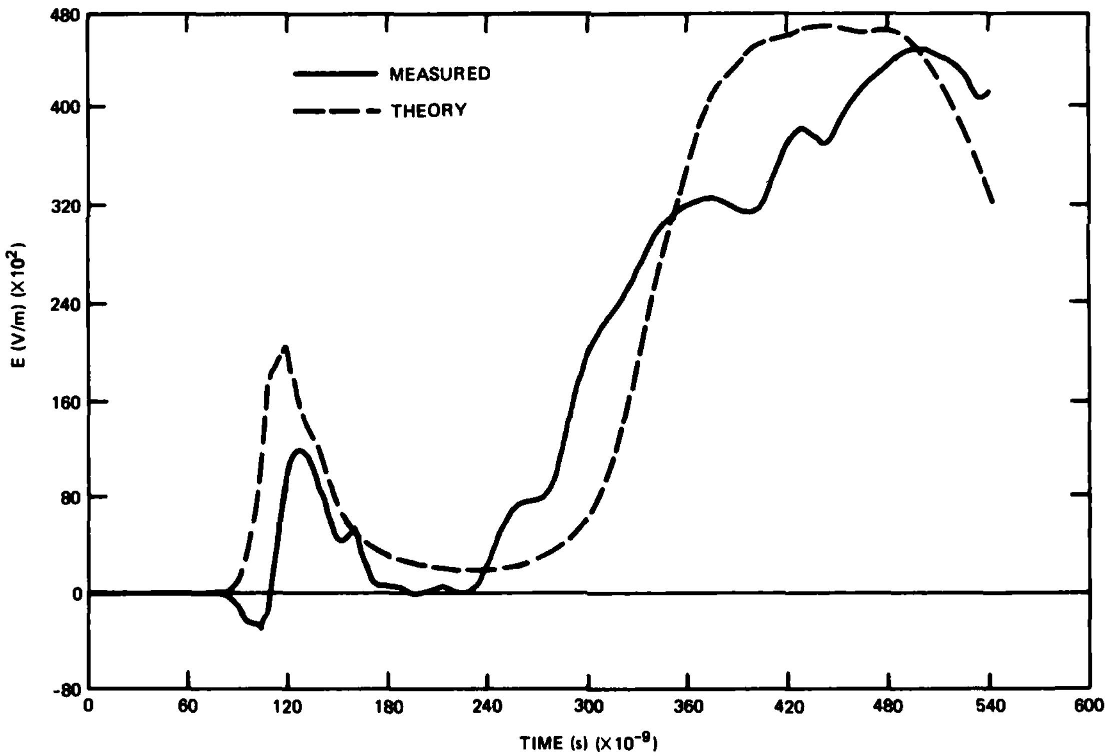

Figure 15. E-field inside parallel-plate transmission line $\left(\sigma_{peak} = 4 \times 10^{-3}\ \text{mho/m}\right)$.

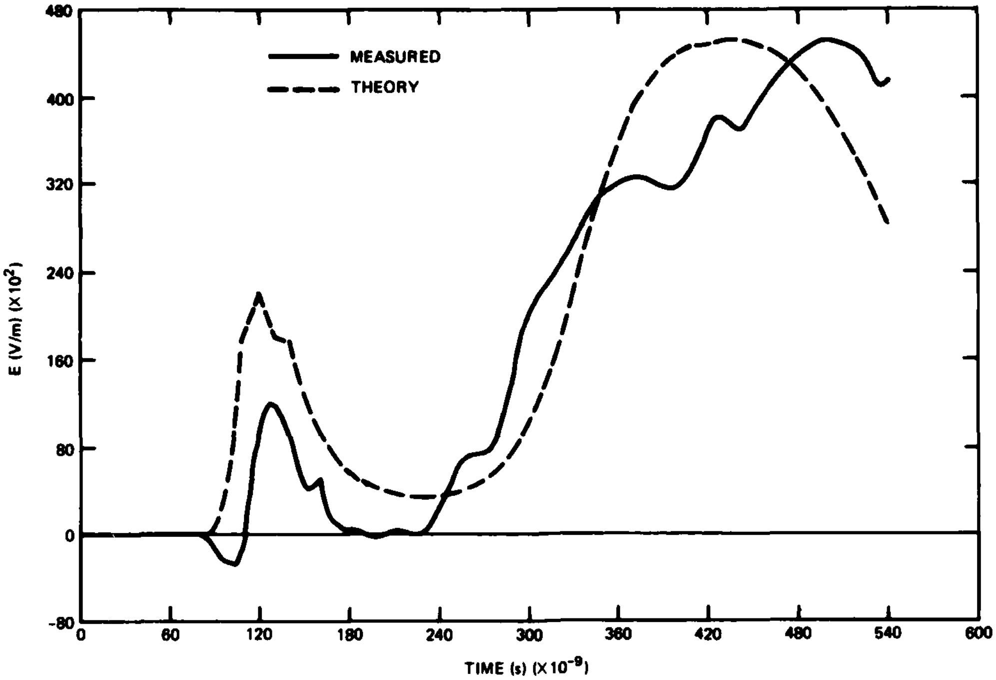

Figure 16. E-field inside parallel-plate transmission line $\left(\sigma_{peak} = 2 \times 10^{-3}\ \text{mho/m}\right)$.

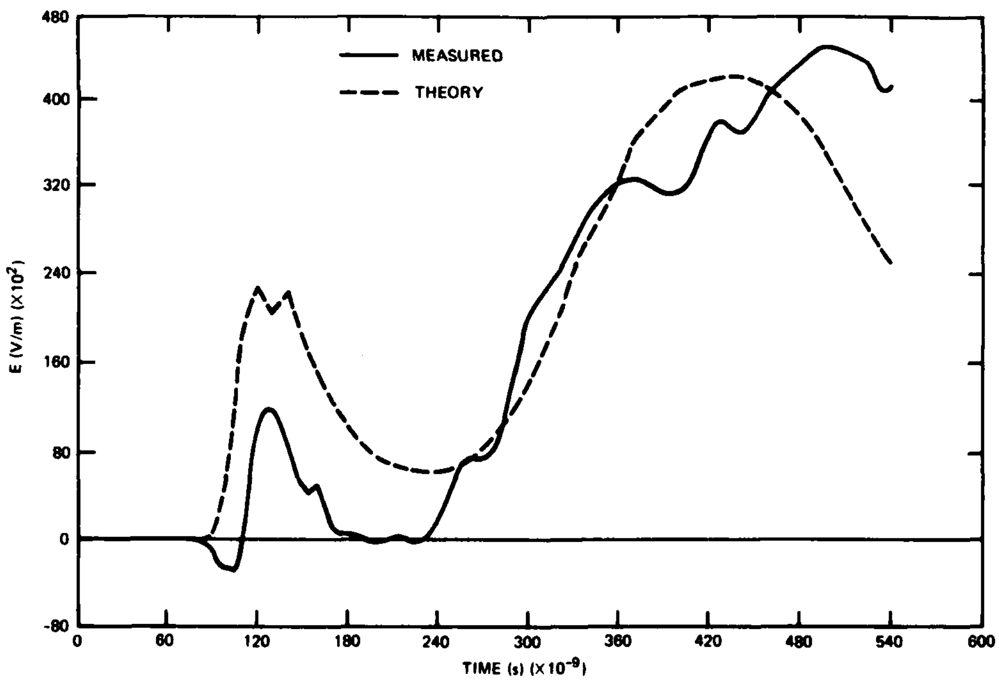

Figure 17. E-field inside parallel-plate transmission line $\left(\sigma_{peak} = 1 \times 10^{-3}\ \text{mho/m}\right)$.

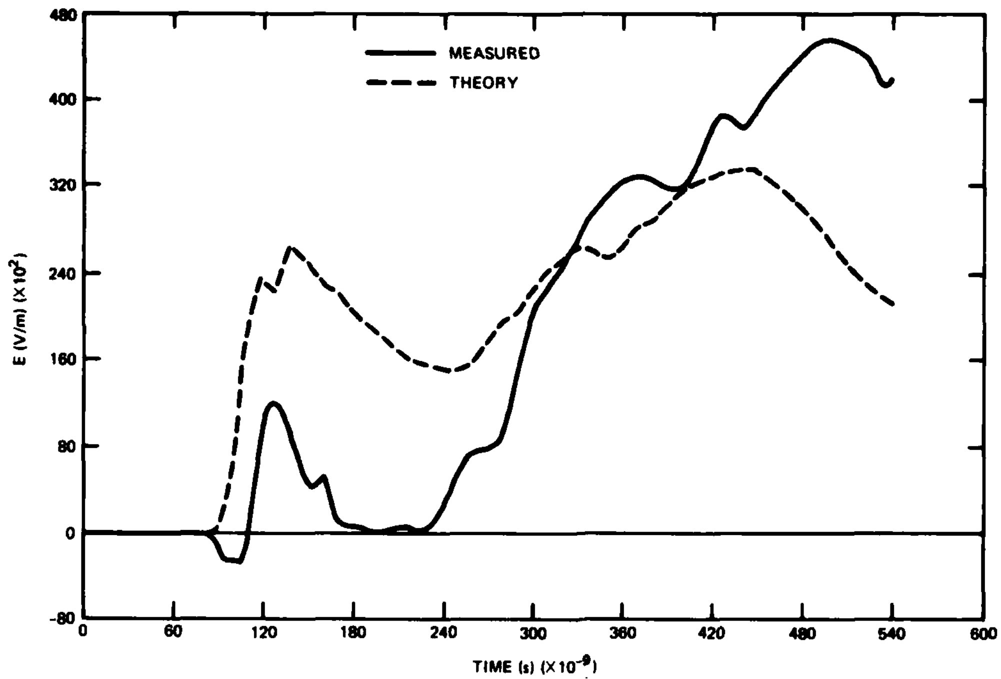

Figure 18. E-field inside parallel-plate transmission line (σ_{peak} = 5.0×10^{-4} mho/m).

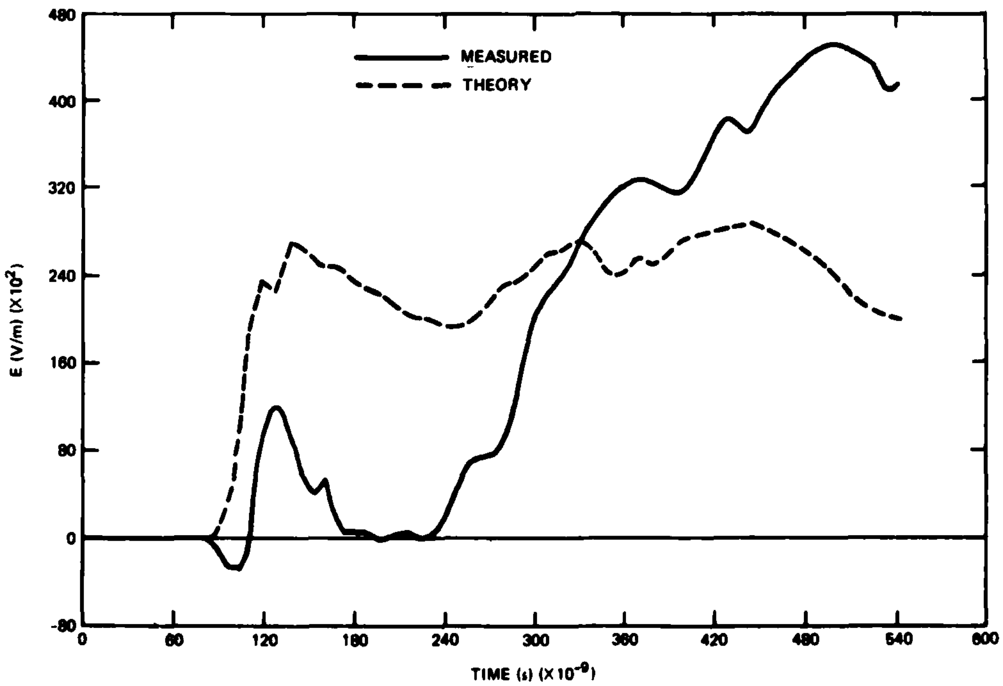

Figure 19. E-field inside parallel-plate transmission line (σ_{peak} = 2.5×10^{-4} mho/m).

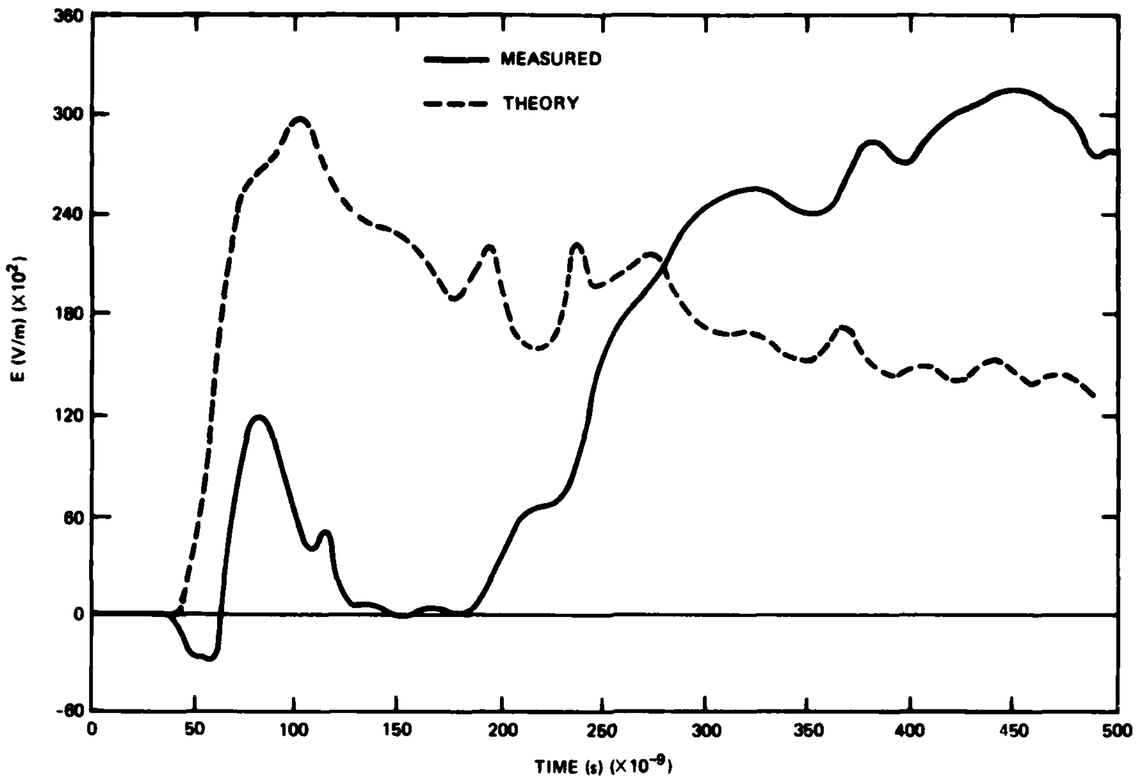

Figure 20. E-field inside parallel-plate transmission line (σ_{peak} = 1.25 × 10^{-4} mho/m).

6. ANTENNA COUPLING EXPERIMENTS AND ANALYSIS

6.1 Experimental Procedures

In a typical test shot procedure, an antenna short-circuit current response was first measured when the parallel-plate line was fired, without firing the AURORA. Next, the measurement was repeated with AURORA and the line firing simultaneously. As already indicated, figure 15 shows a typical E-field measurement obtained with a parallel-plate sensor whose bottom plate is the transmission-line ground plate itself and whose top plate is a round sheet of aluminum foil positioned at a 1/2-in. separation from the ground plate. This sensor has a capacitance of 80 pF and is loaded with a 10-kohm resistor. E-field sensors were placed at three positions in the transmission line. The magnetic field in the parallel-plate transmission line was also measured at the same three positions with Moebius loop magnetic-field sensors. The current flow into the transmission line was also monitored. Unfortunately, because of the large magnitude of current involved, the current probe did not perform up to expectations. A photodiode radiation detector was placed under the transition from the coaxial cable to the parallel-plate transmission line (see fig. 4(a)). The photodiode yielded an absolute value of the radiation dose rate in rads/s. Thirty

to forty thermoluminescent radiation detectors (TLD's)[14] were placed throughout the test cell to monitor the total radiation dose at selected points throughout the room. The transmission line was terminated by a matched load consisting of a curtain of parallel resistor-loaded wires. The current through the curtain was also measured.

To obtain the antenna coupling data presented here, linear monopole antennas of various lengths were mounted horizontally at half-height in the transmission line and shorted to the ground plate. The radiation dose was monitored by four TLD's attached to the antenna, one at the tip, one at the base, and two intermediate. Current response measurements were made with a Singer probe (transfer impedance = 0.1 ohm) mounted around the base of the antenna. The effect of the ionized air on the interaction of the antenna with an incident E-field can be summarized by saying that the air conductivity tends to cause bipolar (oscillatory) responses to become monopolar as a result of the dominance of conductive current (σE) over displacement current $\left(\varepsilon \frac{dE}{dt}\right)$. The oscillations also tend to become damped. The detailed theoretical explanation will be presented in later sections.

6.2 Equivalent Circuit Method

The authors have developed a method of modelling antenna coupling in time-varying conductive air. This method uses equivalent circuit models obtained by established methods.[15] These circuits are modified according to the algorithm described in this section.

Often, the analysis of antennas is undertaken in the frequency domain. This is a natural course of action for dealing with systems whose properties (ε, μ, σ) do not change with time, for in such a case all differential (or integro-differential) equations which arise have time-independent coefficients and kernels. Fourier-transforming these equations converts all time-differential or time-integral operators into simple multipliers, greatly facilitating the analysis. If, in addition to being time-independent, the material properties are also space-independent, the difficulty of the analysis is determined only by the system geometry.

A frequency-domain analysis typically seeks to describe an antenna by two complex functions of frequency--$h(\omega)$ and $Z(\omega)$. The former is the effective height, and describes the antenna's "cross section" (its interaction with its environment). (This environment includes the spatial variation of the electromagnetic driving signal so

---

[14] *Klaus G. Kerris, The AURORA Dosimetry System, Harry Diamond Laboratories, HDL-TR-1754 (March 1976).*

[15] *John Sweton, DNA EMP Handbook, Vol. 2, Coupling Analysis (U), Defense Nuclear Agency, DNA 2114H-2, Ch 10 (July 1979).*

that the effective height would depend, for example, on the angle of incidence of a plane-wave signal.) The latter is the antenna impedance, and describes the antenna's behavior as a circuit element--its interaction with its loading circuit.

A variety of techniques exist for obtaining the effective height and impedance functions. Among these is the "method of the finite-element"[16,17] used by mechanical engineers. The authors have chosen to use this method in their analysis. The effective height and impedance circuits for a vertical monopole--valid for frequencies around and below the first resonance--are shown in figures 21 and 22. These circuit models are consistent with those presented by P. P. Toulios.[18]

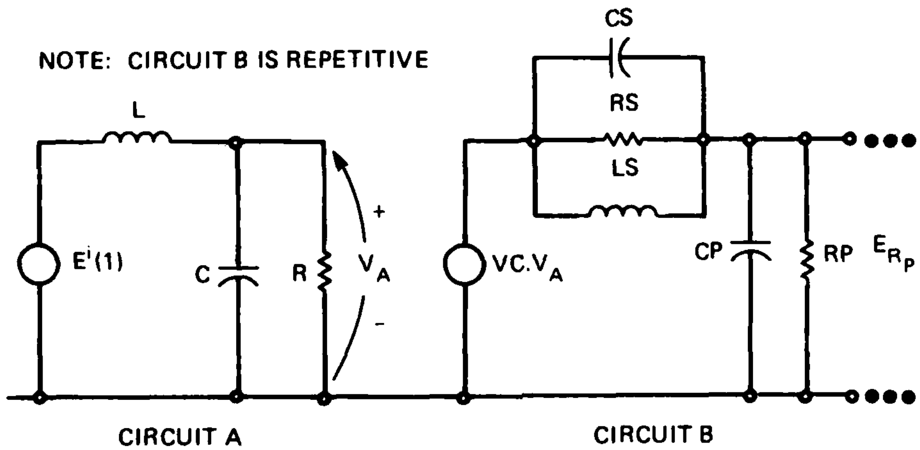

Figure 21. Antenna effective length equivalent circuit for first antenna resonance. Effect of time-varying ambient conductivity on antenna effective height is incorporated into above circuit by inserting time-varying resistor in parallel with each of the three capacitors C_i (i = 1,2,3): $R_i(t) = \varepsilon/[\sigma(t)C_i]$. Equivalent circuits of this type are not limited to simple linear antennas.

[16] *R. F. Harrington, Field Computation by Moment Methods, New York, Macmillan (1968).*

[17] *Hu. H. Chao and Bradley J. Strait, Computer Programs for Radiation and Scattering by Arbitrary Configurations of Bent Wires, Electrical Engineering Dept., Syracuse University, Air Force Cambridge Research Laboratories AFCRL-70-0374 (September 1970). (The Fortran code described by Chao and Strait has been altered so that it can be used for a medium with constant conductivity.)*

[18] *P. P. Toulios, Antenna User's Manual for Linear Cylindrical Antennas in an EMP Environment, Vol. I, IIT Research Institute, DAAG39-72-C-0192 (January 1974).*

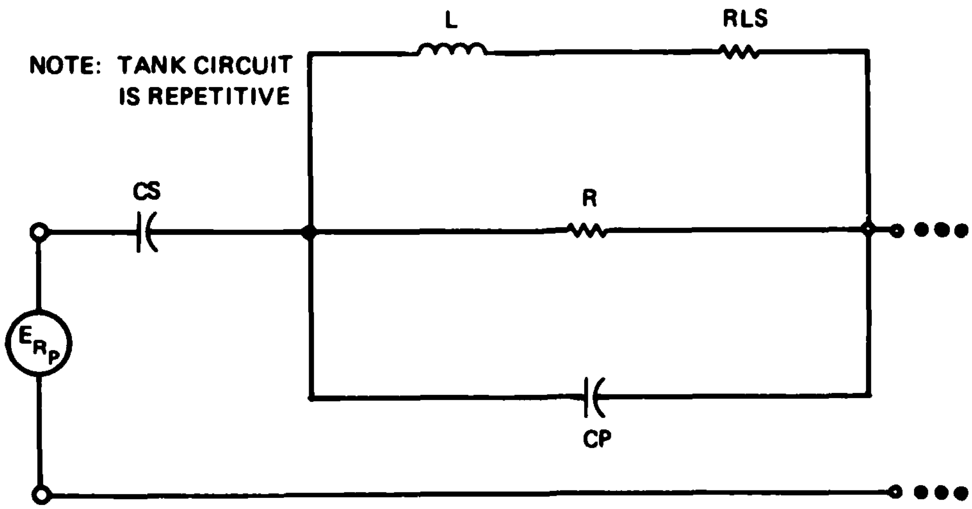

Figure 22. Antenna impedance equivalent circuit for first antenna resonance. Effect of time-varying ambient conductivity on antenna impedance is incorporated into above circuit by inserting time-varying resistor in parallel with each of the two capacitors C_i $(i = 1,2)$: $R_i(t) = \varepsilon/[\sigma(t)C_i]$. Equivalent circuits of this type are not limited to simple linear antennas.

Once $h(\omega)$ and $Z(\omega)$ are found, it is useful to synthesize passive circuits which model the antenna. These circuits serve two purposes: (1) to aid physical intuition and (2) to enable workers to use standard network analysis codes in predicting antenna response. An antenna equivalent circuit can easily be hooked onto, say, a radio circuit to determine the total system response. Equivalent circuit models have been obtained by Toulios for a number of antennas used with Army equipment. These models have proven very useful in dealing with high-altitude EMP signals, but are clearly inappropriate for the source-region case, for which time-varying air conductivity must be taken into account.

Any antenna has a dc capacitance and an infinite set of resonances. It seems intuitively natural to represent this as a Foster canonical circuit.[19,20] Of course, such a representation can only describe a purely reactive system, and must be modified (by the addition of resistors) to include the effects of radiation resistance and of finite air conductivity. (See fig. 23. We ignore antenna and ground

[19] *M. E. Van Valkenburg, Introduction to Modern Network Synthesis, Ch. 5, New York, John Wiley and Sons, Inc. (1967).*

[20] *R. M. Foster, A Reactance Theorem, Bell System Technical Journal, 3 (April 1924), 259-267.*

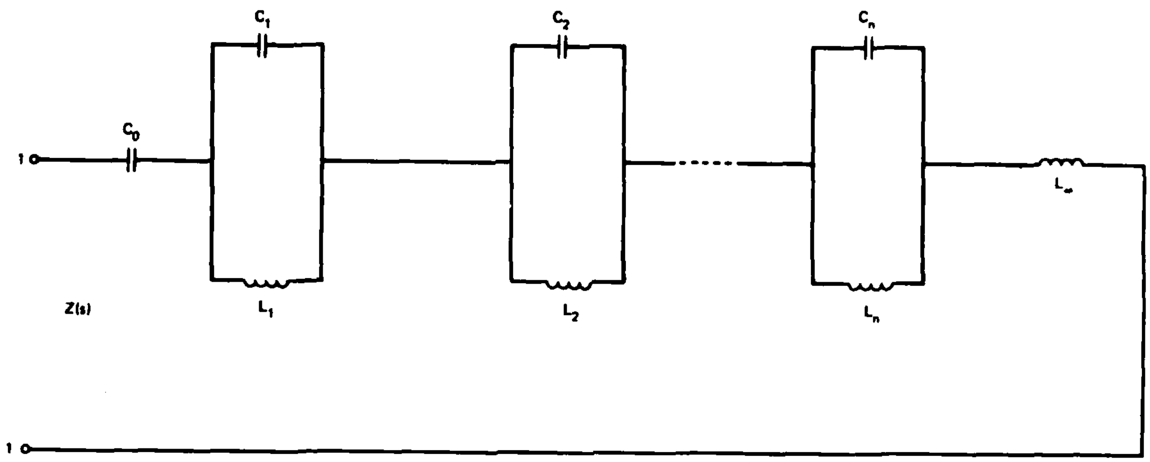

Figure 23. First Foster form of reactive network. C_0 is present if $Z(\omega)$ has pole at $\omega = 0$, and L_∞ is present if $Z(\omega)$ has pole at infinity. After Van Valkenburg (ref. 19).

resistivity.) The resistors which represent air conductivity appear in parallel with each capacitor in the model in accordance with the prescriptive formula: $R = \varepsilon_0/\sigma C$. Thus, a purely capacitive admittance ($Y = i\omega C$) acquires a dissipative term $\left(Y = i\omega C + \frac{1}{R}\right)$. This corresponds to the inclusion of conductive current in the sourceless frequency-domain Maxwell's equations, by the substitution $\varepsilon \to \varepsilon + \frac{\sigma}{i\omega}$. In the language of Faraday lines of force, this means that every E-field line also becomes a current-density line. Thus, both capacitance and conductance contain the same geometrical factor, λ, with dimensions of length

$$C = \lambda\varepsilon$$

$$G = \lambda\sigma$$

$$G = C\,\frac{\sigma}{\varepsilon}\ .$$

The process of network synthesis is considerably simpler for a network containing only two element types (L-C, R-C, or R-L)[21] than for a network containing three element types (L-R-C). In our case, although magnetic, electric, and dissipative mechanisms are all present, we have, in fact (neglecting radiation resistance for the moment), only two element types:

[21] W. Cauer, *Die Verwirklichung von Wechselstromwiderstanden vorgeschriebener Frequenzabhängigkeit*, *Archiv f. Elektrotechnik*, 17 *(1927)*, 355.

1. Inductors--L ($Z = i\omega L$) with impedance $Z_{L_1} = iwl$ and
2. "Repacitors"--(B) with admittance $Y_B = \frac{1}{Z_B} = iwc - G$

$$= iwc \quad 1 - \frac{ij}{\varepsilon\omega} \quad .$$

(The authors have coined the term "repacitor" to denote a hybrid circuit element consisting of a capacitor and resistor connected in parallel. This new term is introduced in preference to, say, "lossy capacitor" in order to emphasize the universality of the medium-dependent factor $\frac{\sigma}{\varepsilon} = \frac{G}{C}$. All capacitors become conductive according to the same ratio, as long as the material parameters are spatially homogeneous.) Clearly, any L-B circuit would reduce, in the case of zero conductivity, to an L-C circuit, and in the case of high conductivity, to an L-R circuit. As long as the medium in which an antenna is embedded is (1) source free and (2) time-invariant, the above considerations apply. This follows from $\varepsilon \to \varepsilon + \frac{\sigma}{i\omega}$ in the Maxwell equations, and hence should correctly model even phenomena arising from finite skin depth in the high σ case. Nor should the inclusion of constant resistors (to model radiation resistance) affect the validity of the capacitor-to-repacitor substitution. Thus, one is tempted to propose the following algorithm for generating the desired circuit model:

(a) Generate (by whatever means) the $h(\omega)$ and $Z(\omega)$ functions for the $\sigma = 0$ case.

(b) Synthesize (by whatever means) circuits which correctly model the $h(\omega)$ and $Z(\omega)$ found in step (a).

(c) Replace all capacitors in (b) by repacitors, according to the formula $C \to C\left(1 - \frac{i\sigma}{\varepsilon\omega}\right)$.

(d) If σ is time-varying, so too will all repacitors become time-varying. (At this point, frequency-domain concepts lose their validity.)

In practice, steps (a) and (b) are very vulnerable to error. It is important to realize that network synthesis is not a unique process. Thus, a circuit which correctly models the $\sigma = 0$ case need not necessarily model the more general $\sigma \neq 0$ case. For instance, small errors in certain capacitors, which might not be apparent in the non-dissipative medium, might lead to large errors when the capacitors become conductive. Thus, steps (a) and (b) should be repeated for a range of constant conductivities between zero and the peak conductivities of interest.

Once it is established that the circuit models the antenna accurately for the time-invariant case, the resistors can be allowed to

vary in time. This approach has yielded very good agreement both with experimental data and finite-difference calculations which numerically solve the Maxwell equations in the neighborhood of the antenna.

In effect, allowing σ to vary in time implies that there are two methods of driving the antenna:

(1) Directly, through the incident electromagnetic field and

(2) Parametrically, through $\sigma(t)$.

The second method is analogous to the behavior of a parametric amplifier, in which the signal modulates a capacitance. Thus, even in an electrostatic field, the antenna can be driven by $\sigma(t)$. Physically, this corresponds to a conduction current source.

Figures 24 to 27 show the effect of time-varying air conductivity on antenna coupling. These figures show measured short-circuit current. Figures 24, 25, and 26 differ in the relative timing of AURORA and the pulser firing and in the magnitude to $\sigma(t)$. Figure 27 shows a measurement with a shorter antenna.

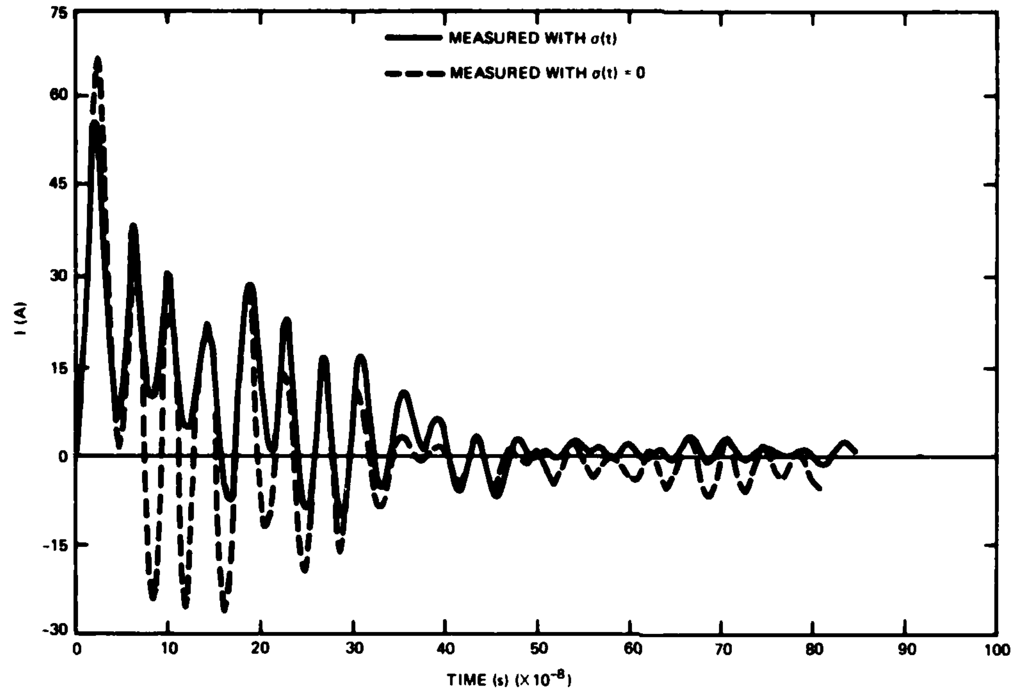

Figure 24. Comparison of measured short-circuit current monopole antenna response (2.42 m) with and without ambient time-varying ionized air conductivity (time in s × 10^{-8}).

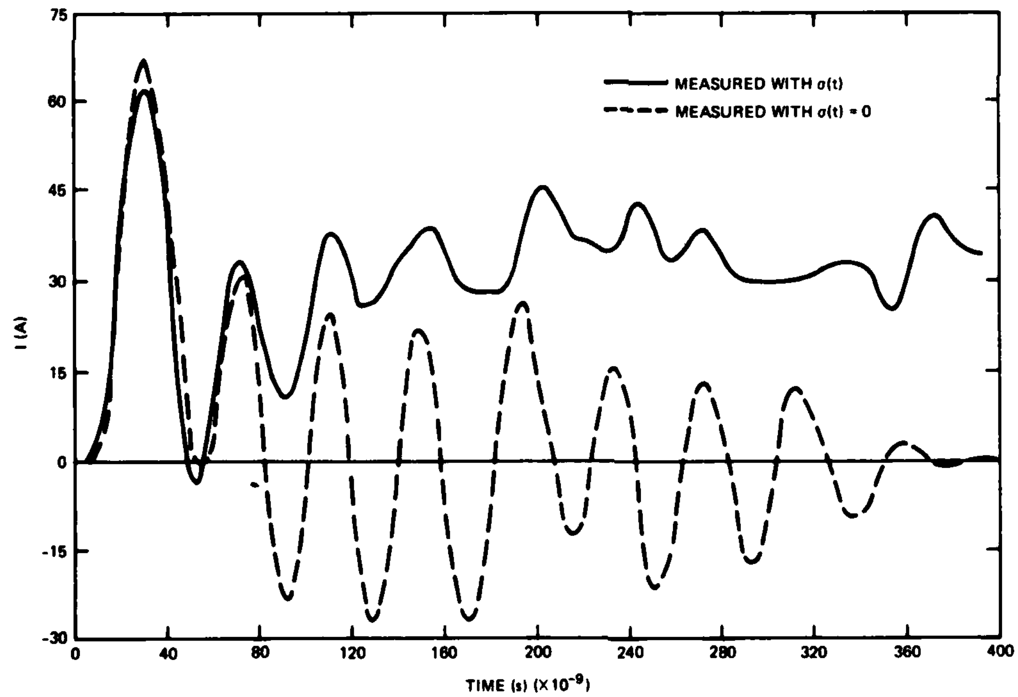

Figure 25. Comparison of measured short-circuit current monopole antenna response (2.42 m) with and without ambient time-varying ionized air conductivity (time in s × 10^{-9}).

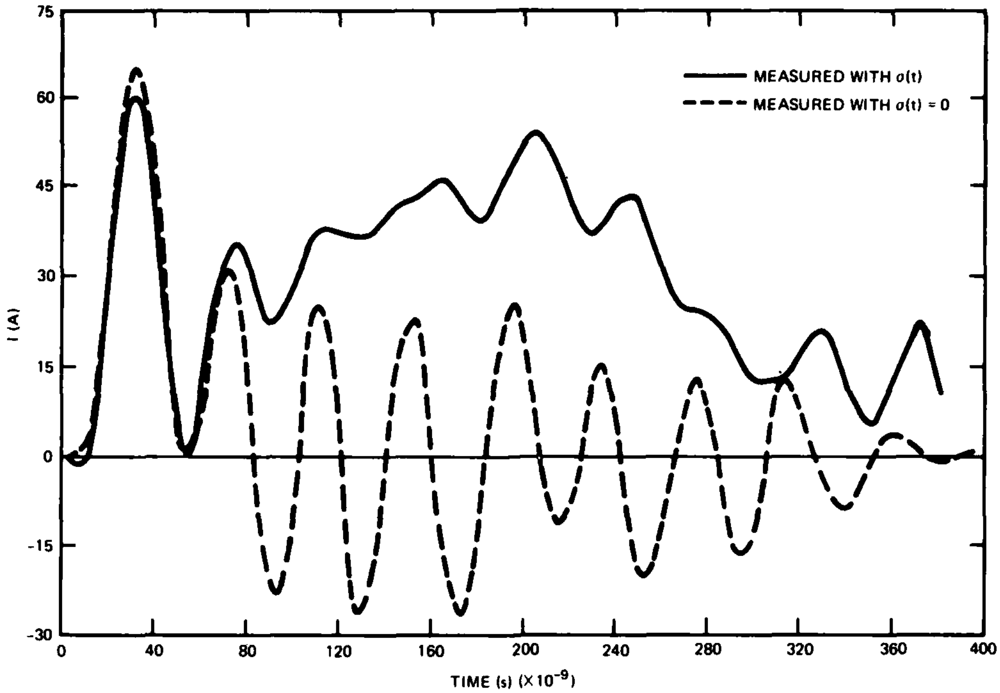

Figure 26. Comparison of measured short-circuit current monopole antenna response (2.42 m) with and without ambient time-varying ionized air conductivity.

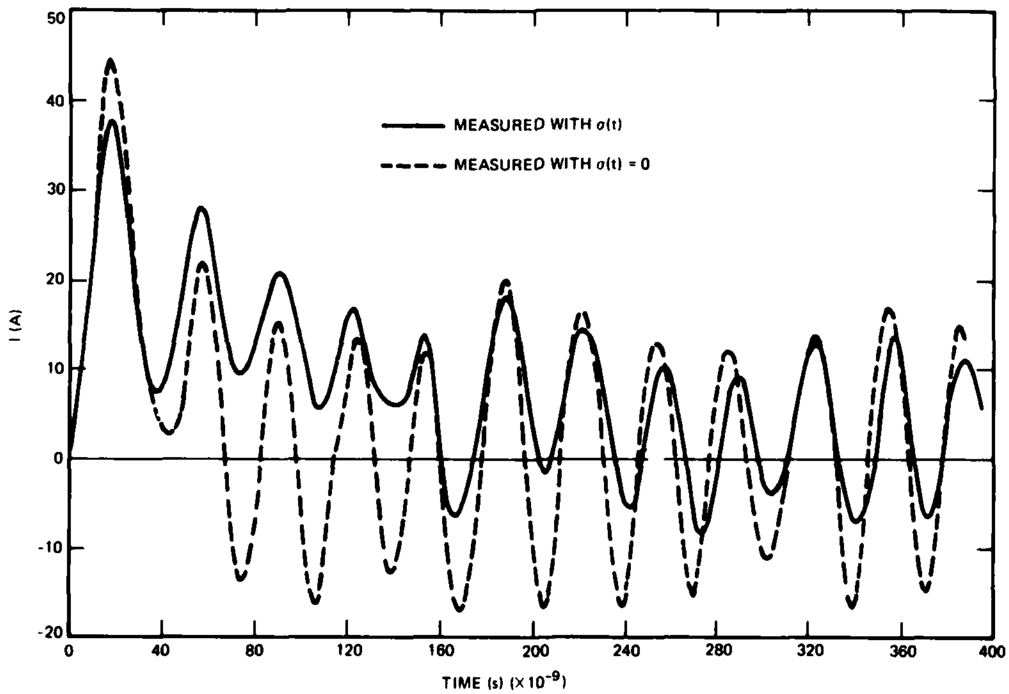

Figure 27. Comparison of measured short-circuit current monopole antenna response (2.21 m) with and without ambient time-varying ionized air conductivity.

6.3 Theoretical Interpretation

The experimental results have been interpreted with two independent calculational approaches. First, the short-circuit current was calculated with a monopole code that numerically calculates the current response from the incident E-field by using Maxwell's equations in finite-difference form with the appropriate boundary conditions. The code, very similar to that developed by Merewether,[22] is a two-dimensional code that takes as input the E-field that would arise in the absence of the antenna. (This formulation has been widely used by the EMP community, but has several significant disadvantages for systems applications. First, the method is appropriate for the solution of simple geometries, but for realistic Army antennas, it can be quite intractable. Similarly, the results of the antenna response obtained by this method are difficult to interface with the frequently used circuit analysis codes--to determine the system response at the component level. This method has obtained respectable results for simple geometries in underground tests and therefore is used here as a basis for judging the validity of the equivalent circuit approach.) Comparisons between calculational and experimental results are shown in figure 28 (without conductivity) and figure 29 (with conductivity).

Next, calculations were made using the LPN equivalent circuit obtained by the algorithm presented in section 6.2. The LPN free-space antenna LPN equivalent circuit models the electrical energy and magnetic energy storage and the dissipative energy loss of the real antenna. Theoretical justification of this approach and a discussion of its limitations are presented more thoroughly in a forthcoming report. Assumptions implicit in the method are that conductivity is independent of field intensity (a good assumption for relative humidity of about 40 percent and fields of less than about 50 kV/m) and spatially homogeneous.

[22] *David E. Merewether, Transient Currents Induced on a Metallic Body of Revolution by an Electromagnetic Pulse, IEEE Trans. EMC,* <u>*EMC-13*</u>*, 2 (May 1971).*

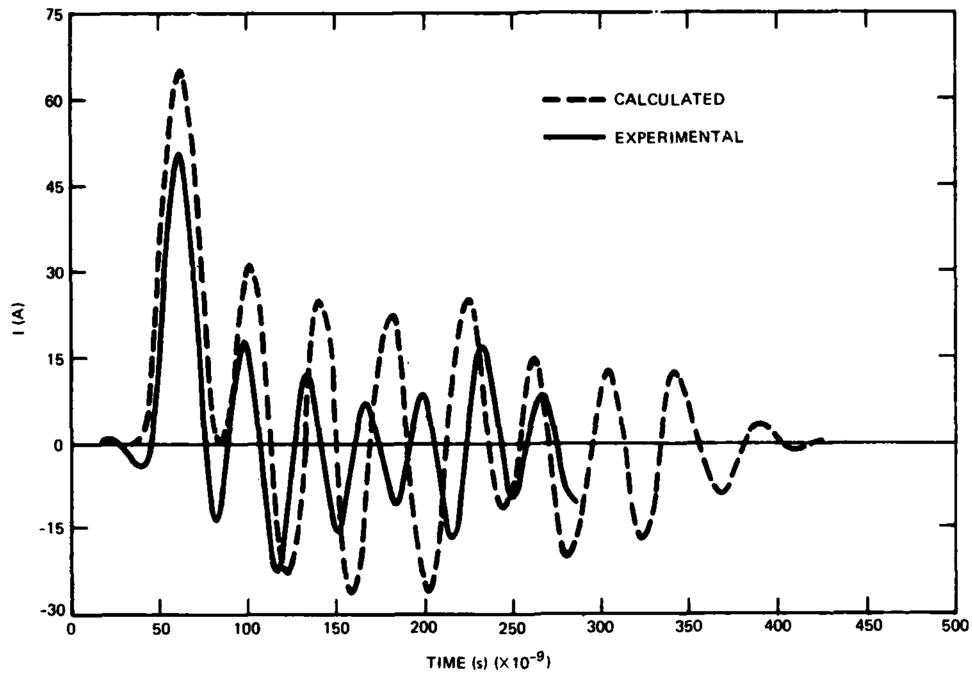

Figure 28. Comparison between experimental antenna short-circuit response and finite difference code calculations of response. No time-varying air conductivity present.

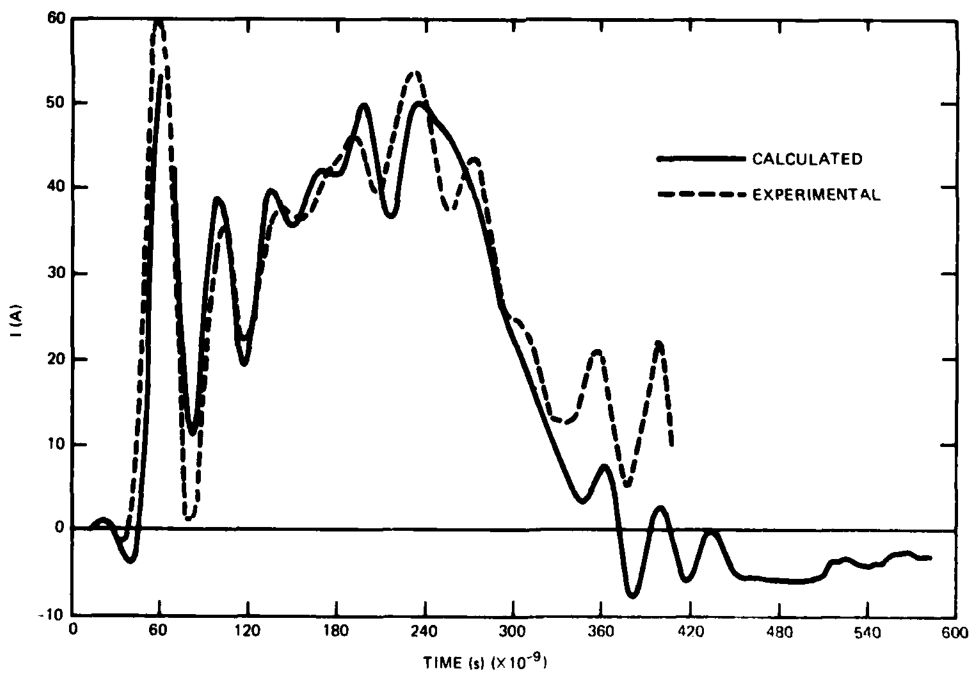

Figure 29. Comparison between experimental antenna short-circuit response and finite difference code calculations of antenna response. Time-varying air conductivity present.

Finally, to complete the cycle, the LPN calculations were compared to the two-dimensional finite difference procedure. Comparisons were made over a wide range of assumptions about conductivity waveforms. Sensitivity of the method to both peak conductivity (always assuming linearity, i.e., $\frac{d\sigma}{dE} = 0$) and high-frequency content of the conductivity waveform were investigated. The comparisons are shown in figure 30 without conductivity and figure 31 with conductivity. There was some doubt about the applicability of the method beyond the "adiabatic regime," where $\sigma(t)$ varies slowly in comparison with the driving fields. Figure 32 compares Merewether's finite-difference

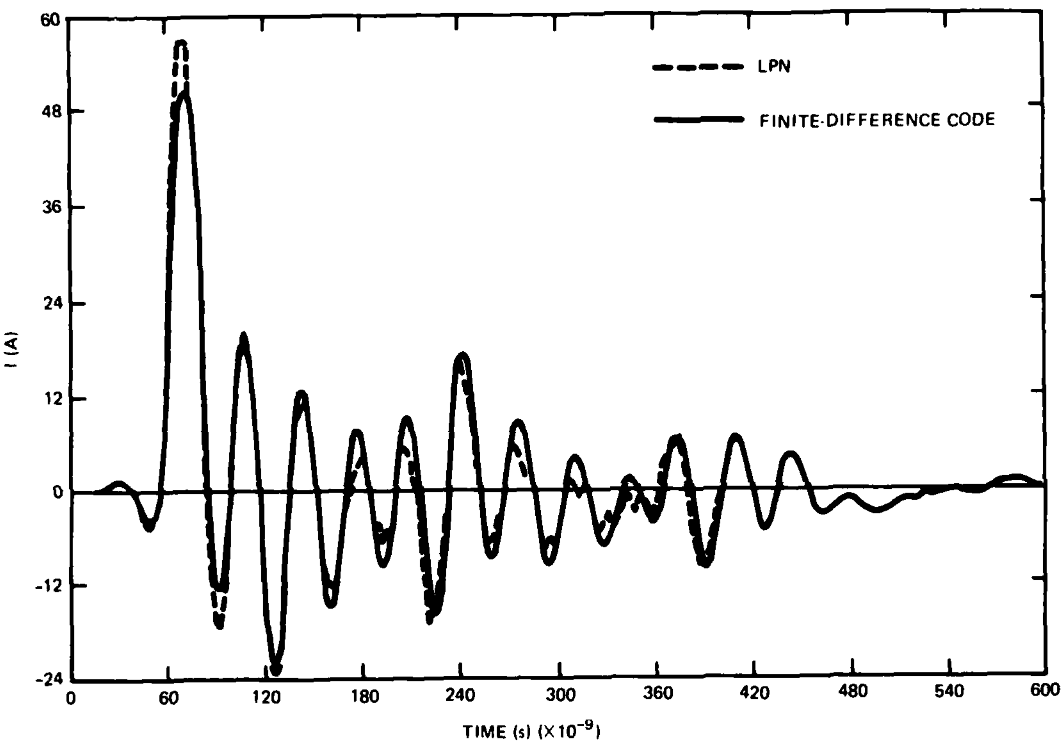

Figure 30. Comparison between LPN and finite difference code response calculations. No time-varying air conductivity present.

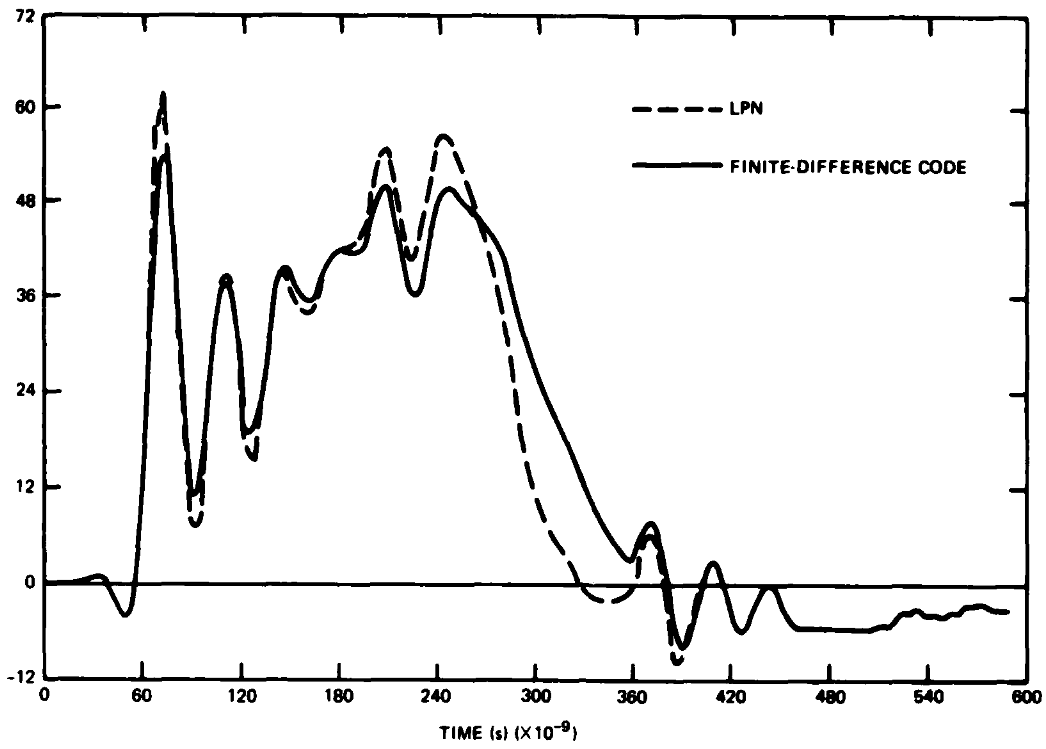

Figure 31. Comparison between LPN and finite difference code response calculations. Time-varying air conductivity present.

calculational procedure with the lumped-parameter equivalent circuit method for E(t) and $\sigma(t)$ of the same shape--a distinctly nonadiabatic condition. Normalization of $\sigma(t)$ was chosen so that the peak conductivity was 4×10^{-3} mho/m. Agreement is remarkably good.

Thus, a three-way agreement has been established between (1) experiment, (2) a finite-difference method, and (3) a lumped-parameter equivalent circuit method. Experimental results have also been obtained for more general antennas--capacitively and inductively loaded linear antennas, loop antennas, and helical antennas. The authors feel that the lumped-parameter method can be successfully generalized to accommodate these configurations.

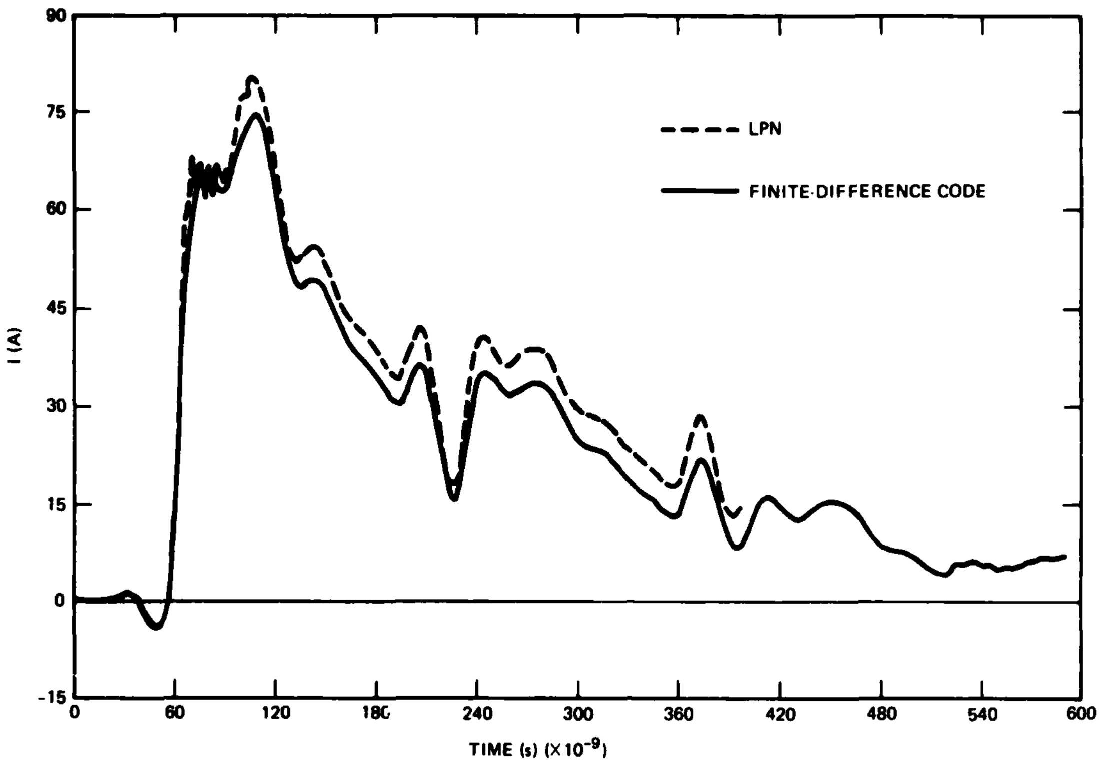

Figure 32. Comparison between LPN and finite difference code response calculations. Normalized form of time-varying air conductivity time history is assumed to be same as normalized time history of incident electric field. This calculation was carried out to check LPN antenna equivalent circuit for situations in which time-varying conductivity varied very rapidly.

7. LIMITATIONS

7.1 Experimental Apparatus

Many limitations of the experimental approach have been mentioned in the previous discussions but, for the sake of clarity, they are further highlighted here.

First, AURORA produces a conductivity time history whose rise rate is slower than desired.

The parallel-plate transmission line has several drawbacks for this type of application. First, the volume available for testing (the region between the plates) is limited, since the line must be placed in the AURORA test chamber. The plate separation cannot be too great because of the effect of the test chamber's conducting walls. Furthermore, in order to successfully launch an electromagnetic wave down the line, it must be fed from a point through a tapered transition section before it reaches the parallel section. This tapered region cannot be used for testing, yet it consumes a rather large section of the limited available space. In addition, the parallel-plate line must be terminated in such a way as to prevent a reflected wave from returning to the paralleled test section. A conventional way of doing this is by tapering the line and installing a resistor which has the value of the characteristic impedance of the parallel-plate line. For our experiment, in order to have the parallel section as long as possible, the termination taper section was omitted and the transmission line was terminated abruptly in an "anechoic curtain" of parallel anu series resistors. Even though the total terminating resistance approximated that of the line, the abrupt geometry change resulted in some reflected signal (approximately 5 percent). Although not considered significant, its presence must be recognized.

As previously discussed, the parallel-plate line itself is affected by the presence of the conductivity, which tends to "short out" the field in the line. A related effect that is present has been called the "inductive kick." This is a sudden rise in the electric field after the conductivity is removed. It is present because of the inherent inductance of the line. This "shorting out" and "inductive kick" behavior is a manifestation of the experimental setup and not really related to the threat environment. However, as described earlier, the authors are confident that these effects can be greatly reduced.

Objects placed in the line can also perturb its behavior. For instance, the long antenna stretching nearly from plate to plate

distorts the current in the hot plate, or equivalently induces an image antenna.[23] We have established, through analysis with the monopole code, that this effect is negligible for the cases we considered.

Another effect which is present and must be addressed is the boundary layer. Since electrons are not easily emitted from a metal surface, yet are highly mobile in an ionized gas, negatively charged metallic surfaces exposed to a radiation environment such as AURORA become surrounded by an electron depletion layer. This affects the electromagnetic coupling. In the case of these experiments, the effect can be ignored because of properties of air and the geometry. However, in the event that experiments dealing with smaller geometries such as electronic circuit elements or some other medium are attempted, the effect may be pronounced.

Another thing that must be highlighted concerns the nature of the experiments that have been conducted. The experiments and test apparatus were designed to consider only the response of gamma-thin objects (objects which are thin with respect to a gamma path length and, therefore, do not experience any direct charge buildup due to the radiation). This, then, allows one to make the approximation that the environment and the coupling are separable; that is, one can assume that the field which would exist without the system (or antenna) present is the incident field which is then coupled to the system. To treat the gamma thick problem[24] (which might be more realistic when considering all Army systems) would be considerably more difficult.

Another effect which is present in the actual threat situation is that of neutrons. The neutrons undergo inelastic scattering as well as capture and result in further late-time sources of gamma radiation. This effect has been totally ignored. This assumption is probably not too severe because it is both of lower magnitude and later in time and probably has little effect on the short antennas considered here--even though it must be considered a limitation of the general application of this scheme.

When viewed in the context of experimental verification of analytical models, the experimental configuration can be considered successful. This is not to say that the LAEMP environment has been

---

[23]*Clayborne D. Taylor, George A. Steigerwald, On the Pulse Excitation of a Cylinder in a Parallel Plate Wave Guide, Mississippi State University, Sandia Laboratories Sensor and Simulation Note 99, Vol. 7 (March 1970).*

[24]*G. Merkel, D. J. Spohn, C. L. Longmire, and W. F. Crevier, An Equivalent-Circuit Analysis of the HDL Concentric Cylinder Experiments in AURORA, IEEE Trans Nucl Sci, NS-24, 6 (December 1977).*

simulated in the sense that in order to demonstrate system survivability one need only expose the system to its environment and then demonstrate that the system remains functional. This was not the goal of the experiment and should not be interpreted as a result.

7.2 Equivalent Circuit Model

There are several well-known limitations of equivalent-circuit models (such as frequency limitations) which, of course, apply to the formulation presented here. In addition to these conventional limitations, this model demands that the conductivity be spatially homogeneous (even though it could be generalized to nonhomogeneous situations, as illustrated by the transmission-line model presented in section 4.1).

In a related issue, the coupling to antennas is naturally a function of the driving field. Uncertainties in the environment (particularly the late-time air chemistry) will cast a similar doubt on the antenna coupling.

8. CONCLUSIONS AND EXPECTED FOLLOW-ON WORK

The authors feel that considerable progress has been made in the understanding of source-region EMP coupling. This progress has taken the form of advances both in experimental techniques and analytical and numerical modelling. Certain simplifying assumptions were essential to the development of these techniques. As is often required in research, many simultaneous effects must be isolated from one another in order to gain understanding.

In the work reported here, attention was concentrated on the effect of time-varying air conductivity on EMP coupling. Tactical environmental components which were temporarily neglected in both experimental design and analysis were the following.

(1) All effects of local Compton currents (system charging, space charging, spatial inhomogeneities in $\sigma(t)$).

(2) All neutron effects.

(3) Boundary layers formed at metallic surfaces due to electron depletion in high surface fields.

(4) Avalanching in high surface fields.

(5) Nonlinearity (E-field dependence) of $\sigma(t)$.

The transmission-line simulation produced excellent results, despite some undesirable effects, i.e., line-AURORA interaction and line-antenna interaction. These loading effects can and will be minimized in future experiments, probably using techniques described above (sect. 4).

The measurements of source-region antenna coupling were very instructive, and have been nicely modelled by the equivalent-circuit method described in this paper. In obtaining experimental data, the authors turned to AURORA as a source of large-volume ionizing radiation, and were constrained as a result of a certain conductivity waveform whose rise-rate was not ideal (too slow). However, developments in pulsed power--at HDL (per Alexander Stewart)* and elsewhere--lead us to believe that better sources will become available. In any case, comparisons between substantially different theoretical methods imply that our equivalent-circuit treatment can be generalized to the case of faster-varying conductivity.

The most dramatic effect of time-varying conductivity is that conductive current (σE) dominates displacement current $\left(\epsilon \frac{dE}{dt}\right)$ in driving an antenna with a low-impedance load. Whereas the displacement current driver tends to excite resonances, the conduction current driver tends to be low frequency and monopolar.

The master-slave transmission-line approach must be developed for investigating electromagnetic coupling in time-varying air conductivity. The use of a highly ionizable gas, such as N_2, may make the technique suitable for source-region strategic EMP research.

The authors also expect to continue to study the behavior of ionized gases at various pressures, in an attempt to relate macroscopic (linear and nonlinear conductivity) and microscopic (plasma frequency, collision frequency, attachment and recombination rates, avalanching, etc.) parameters. Appropriate experimental approaches may include capacitive probes, "pie-pans," and microwave propagation techniques.[25] For example, nonlinear conductivity could be studied by looking for frequency-doubling in microwave signals.

The equivalent-circuit antenna analysis method will be applied to more general antenna types, such as loops and log-periodic antennas. The technique applies whenever $\sigma(t)$ is spatially homogeneous. Techniques for spatially inhomogeneous environments must be developed, if gamma-thick objects in the source region are to be treated.

The authors are developing a similar series of code verification experiments for communication cables exposed to the threat criteria

[25] *C. E. Baum, Some Limitations on Microwave Air-Conductivity Measurements, Electromagnetic Pulse Sensor and Simulation Notes, Vol. I, Note 16 (June 1970).*

**A. Stewart, Harry Diamond Laboratories, private communication.*

environment. This effort presents more of a challenge since the orientation of the field, presence of the ground, and lengths involved all must be treated differently than the simple antenna. Nevertheless, initial indications are that a sufficiently good simulation can be accomplished to at least verify the coupling codes for the simplest configurations.

LITERATURE CITED

(1) Nuclear Survivability Criteria for Army Tactical Equipment (U), U.S. Army Nuclear Agency, NUA-C-5400-74 (August 1974). (CONFIDENTIAL-RESTRICTED DATA)

(2) Hans Fleischmann, High Current Electron Beams, Physics Today, 28, 5 (May 1975), 34.

(3) Gerold Yonas, Fusion Power with Particle Beams, Scientific American, (November 1978), 50.

(4) B. Bernstein and I. Smith, AURORA, An Electron Accelerator, IEEE Trans Nucl Sci, NS-20, 3 (June 1973).

(5) L. M. Anderson et al, Status of AURORA Environment Calculations, IEEE Trans Nucl Sci, NS-25, 6 (December 1978).

(6) R. Manriquez, G. Merkel, W. D. Scharf, and D. Spohn, Electrically Short Monopole Antenna Response in an Ionized Air Environment--Determination of Ionized Air Conductivity, IEEE Trans Nucl Sci, 26, 6 (December 1979).

(7) W. F. Crevier, C. L. Longmire, G. Merkel, D. J. Spohn, Air Chemistry and Boundary Layer Studies with AURORA, IEEE Trans Nucl Sci, NS-24, 6 (December 1977).

(8) Dean L. May, Electron Mobility and Electron Attachment Rate in an Electromagnetic Pulse Air Environment, Harry Diamond Laboratories Student Technical Symposium (17 to 18 August 1977), 87.

(9) R. Manriquez, G. Merkel, and D. Spohn, Modification of the AURORA Environment, Harry Diamond Laboratories, HDL-PR-79-5 (October 1979).

(10) R. Manriquez, G. Merkel, and D. Spohn, Modification of the AURORA Electromagnetic Environment, IEEE Annual Conference on Nuclear and Space Radiation Effects (July 1978).

(11) H. J. Longley and C. L. Longmire, Electron Mobility and Attachment Rate in Moist Air, Mission Research Corporation, MRC-N-222 (1975).

(12) C. E. Baum, The Calculation of Conduction Electron Parameters in Ionized Air, Electromagnetic Pulse Theoretical Notes, I, Note 6 (May 1967).

(13) M. Bushell, R. Manriquez, G. Merkel, W. Scharf, and D. Spohn, Source-Region EMP Simulator--A Parallel Plate Transmission Line in the AURORA Test Cell, IEEE Trans Nucl Sci, NS-27, 6 (December 1980).

(14) Klaus G. Kerris, The AURORA Dosimetry System, Harry Diamond Laboratories, HDL-TR-1754 (March 1976).

(15) John Sweton, DNA EMP Handbook, Vol. 2, Coupling Analysis (U), Defense Nuclear Agency, DNA 2114H-2, Ch 10 (July 1979).

(16) R. F. Harrington, Field Computation by Moment Methods, New York, Macmillan (1968).

(17) Hu. H. Chao and Bradley J. Strait, Computer Programs for Radiation and Scattering by Arbitrary Configurations of Bent Wires, Electrical Engineering Dept., Syracuse University, Air Force Cambridge Research Laboratories AFCRL-70-0374 (September 1970). (The Fortran code described by Chao and Strait has been altered so that it can be used for a medium with constant conductivity.)

(18) P. P. Toulios, Antenna User's Manual for Linear Cylindrical Antennas in an EMP Environment, Vol. I, IIT Research Institute, DAAG39-72-C-0192 (January 1974).

(19) M. E. Van Valkenburg, Introduction to Modern Network Synthesis, Ch. 5, New York, John Wiley and Sons, Inc. (1967).

(20) R. M. Foster, A Reactance Theorem, Bell System Technical Journal, 3 (April 1924), 259-267.

(21) W. Cauer, Die Verwirklichung von Wechselstromwiderstanden vorgeschriebener Frequenzabhängigkeit, Archiv f. Elektrotechnik, 17 (1927), 355.

(22) David E. Merewether, Transient Currents Induced on a Metallic Body of Revolution by an Electromagnetic Pulse, IEEE Trans. EMC, EMC-13, 2 (May 1971).

(23) Clayborne D. Taylor, George A. Steigerwald, On the Pulse Excitation of a Cylinder in a Parallel Plate Wave Guide, Mississippi State University, Sandia Laboratories Sensor and Simulation Note 99, Vol. 7 (March 1970).

(24) G. Merkel, D. J. Spohn, C. L. Longmire, and W. F. Crevier, An Equivalent-Circuit Analysis of the HDL Concentric Cylinder Experiments in AURORA, IEEE Trans Nucl Sci, NS-24, 6 (December 1977).

(25) C. E. Baum, Some Limitations on Microwave Air-Conductivity Measurements, Electromagnetic Pulse Sensor and Simulation Notes, Vol. I, Note 16 (June 1970).

DISTRIBUTION

ADMINISTRATOR
DEFENSE TECHNICAL INFORMATION CENTER
ATTN DTIC-DDA (12 COPIES)
CAMERON STATION, BUILDING 5
ALEXANDRIA, VA 22314

COMMANDER
US ARMY RSCH & STD GP (EUR)
ATTN CHIEF, PHYSICS & MATH BRANCH
FPO NEW YORK 09510

COMMANDER
US ARMY ARMAMENT MATERIEL
READINESS COMMAND
ATTN DRSAR-LEP-L, TECHNICAL LIBRARY
ATTN DRSAR-ASF, FUZE & MUNITIONS
SUPPORT DIV
ROCK ISLAND, IL 61299

COMMANDER
US ARMY MISSILE & MUNITIONS
CENTER & SCHOOL
ATTN ATSK-CTD-F
REDSTONE ARSENAL, AL 35809

DIRECTOR
US ARMY MATERIEL SYSTEMS ANALYSIS
ACTIVITY
ATTN DRXSY-MP
ABERDEEN PROVING GROUND, MD 21005

DIRECTOR
US ARMY BALLISTIC RESEARCH LABORATORY
ATTN DRDAR-TSB-S (STINFO)
ABERDEEN PROVING GROUND, MD 21005

US ARMY ELECTRONICS TECHNOLOGY
& DEVICES LABORATORY
ATTN DELET-DD
FT MONMOUTH, NJ 07703

HQ, USAF/SAMI
WASHINGTON, DC 20330

TELEDYNE BROWN ENGINEERING
CUMMINGS RESEARCH PARK
ATTN DR. MELVIN L. PRICE, MS-44
HUNTSVILLE, AL 35807

COMMANDING OFFICER
NAVAL TRAINING EQUIPMENT CENTER
ATTN TECHNICAL LIBRARY
ORLANDO, FL 32813

PROJECT OFFICER
PHYSICAL SECURITY EQUIPMENT
7500 BACKLICK ROAD, BUILDING 3089
SPRINGFIELD, VA 22150

ENGINEERING SOCIETIES LIBRARY
ATTN ACQUISITIONS DEPARTMENT
345 EAST 47TH STREET
NEW YORK, NY 10017

TEXAS INSTRUMENTS, INC
PO BOX 226015
ATTN FRANK POBLENZ
DALLAS, TX 75266

RELIABILITY ANALYSIS CENTER
RADC (RBRAC)
ATTN DATA COORDINATOR/GOVT PROGRAMS
GRIFFISS AFB, NY 13441

ANALYTICAL SYSTEMS ENGINEERING CORP
OLD CONCORD ROAD
ATTN LIBRARIAN
BURLINGTON, MA 01803

AMES LABORATORY
DEPT OF ENERGY
IOWA STATE UNIVERSITY
ATTN ENVIRONMENTAL SCIENCES
ATTN HIGH ENERGY PHYSICS
ATTN EXPERIMENTAL NUCLEAR
ATTN SOLID STATE PHYSICS
ATTN NUCLEAR SCIENCE CATEGORY
AMES, IA 50011

BROOKHAVEN
DEPT OF ENERGY
ASSOCIATED UNIVERSITIES, INC
ATTN TECHNICAL INFORMATION DIV
ATTN PHYSICS DEPT, 5103
UPTON, LONG ISLAND, NY 11973

DEPARTMENT OF COMMERCE
NATIONAL BUREAU OF STANDARDS
ATTN LIBRARY
WASHINGTON, DC 20234

DEPARTMENT OF COMMERCE
NATIONAL BUREAU OF STANDARDS
CENTER FOR RADIATION RESEARCH
WASHINGTON, DC 20234

US DEPT OF ENERGY
ASSISTANT SECRETARY FOR NUCLEAR ENERGY
WASHINGTON, DC 20585

DEPARTMENT OF ENERGY
ALBUQUERQUE OPERATIONS OFFICE
PO BOX 5400
ALBUQUERQUE, NM 87115

NATIONAL COMMUNICATIONS SYSTEM
OFFICE OF THE MANAGER
ATTN LIBRARY
WASHINGTON, DC 20305

NATIONAL OCEANIC & ATMOSPHERIC ADM
ENVIRONMENTAL RESEARCH LABORATORIES
ATTN LIBRARY, R-51, TECH REPORTS
BOULDER, CO 80302

INSTITUTE FOR TELECOMMUNICATIONS
SCIENCES
NATIONAL TELECOMMUNICATIONS
& INFO ADMIN
ATTN LIBRARY
BOULDER, CO 80303

DIRECTOR
DEFENSE ADVANCED RESEARCH
PROJECTS AGENCY
ARCHITECT BLDG
ATTN MATERIALS SCIENCES
ATTN ADVANCED CONCEPTS DIV
ATTN TARGET ACQUISITION
& ENGAGEMENT DIV
ATTN WEAPONS TECH & CONCEPTS DIV
1400 WILSON BLVD
ARLINGTON, VA 22209

DIRECTOR
DEFENSE COMMUNICATIONS AGENCY
ATTN TECH LIBRARY
ATTN COMMAND AND CONTROL TECHNICAL
CENTER
WASHINGTON, DC 20305

DIRECTOR
DEFENSE COMMUNICATIONS ENGINEERING
CENTER
ATTN TECHNICAL LIBRARY
1860 WIEHLE AVE
RESTON, VA 22090

DIRECTOR
DEFENSE INTELLIGENCE AGENCY
ATTN DT-1, NUCLEAR & APPLIED
SCIENCES DIV
ATTN DT-2, WEAPONS & SYSTEMS DIV
ATTN DT-4, ELECTRONICS & COMMAND
& CONTROL DIV
WASHINGTON, DC 20301

CHAIRMAN
JOINT CHIEFS OF STAFF
ATTN J-3, ELECTRONIC WARFARE DIV
ATTN J-5, NUCLEAR DIV
WASHINGTON, DC 20301

DIRECTOR
NATIONAL SECURITY AGENCY
ATTN TECHNICAL LIBRARY
FT MEADE, MD 20755

DIRECTOR
DEFENSE NUCLEAR AGENCY
ATTN DDST, E. E. CONRAD, DEP DIR
SCIENCE & TECHNOLOGY
ATTN TISI, SCIENTIFIC INFORMATION DIV
ATTN TITL, TECHNICAL LIBRARY DIV
ATTN SPTD, TEST DIVISION
ATTN RAAE, ATMOSPHERIC EFFECTS DIV
ATTN RAEV, ELECTRONICS
VULNERABILITY DIV
ATTN RAEE, EMP EFFECTS DIV
WASHINGTON, DC 20305

COMMANDER
FIELD COMMAND
DEFENSE NUCLEAR AGENCY
ATTN FCPR
ATTN FCSD-A4, TECH REF BR
KIRTLAND AFB, NM 87115

CHIEF
FIELD COMMAND
DEFENSE NUCLEAR AGENCY
LIVERMORE DIVISION
PO BOX 808
ATTN FCPRL
LIVERMORE, CA 94550

DIRECTOR
ARMED FORCES RADIOBIOLOGY
RESEARCH INSTITUTE
DEFENSE NUCLEAR AGENCY
NATIONAL NAVAL MEDICAL CENTER
BETHESDA, MD 20014

UNDER SECRETARY OF DEFENSE
FOR RESEARCH & ENGINEERING
ATTN TEST & EVALUATION
ATTN RESEARCH & ADVANCED TECH
WASHINGTON, DC 20301

OUSDR&E
DIRECTOR ENERGY TECHNOLOGY OFFICE
THE PENTAGON
WASHINGTON, DC 20301

OUSDR&E
ASSISTANT FOR RESEARCH
THE PENTAGON
WASHINGTON, DC 20301

ASSISTANT TO THE SECRETARY OF DEFENSE
ATOMIC ENERGY
ATTN EXECUTIVE ASSISTANT
WASHINGTON, DC 20301

OFFICE OF THE ASSISTANT
SECRETARY OF DEFENSE
PROGRAM ANALYSIS & EVALUATION
ROOM 2E313, THE PENTAGON
WASHINGTON, DC 20301

OFFICE, DEPUTY CHIEF OF STAFF
FOR OPERATIONS & PLANS
DEPT OF THE ARMY
ATTN DAMO-RQC, TELECOM CMD
& CONTROL DIV
WASHINGTON, DC 20310

ASSISTANT CHIEF OF STAFF
FOR INTELLIGENCE
DEPT OF THE ARMY
WASHINGTON, DC 20310

ASSISTANT SECRETARY OF THE ARMY
RES, DEV, & ACQ
ATTN DEP FOR SCI & TECH
ATTN DEP FOR COMMUNICATIONS
& TARGET ACQUISITION
WASHINGTON, DC 20310

DIRECTOR
APPLIED TECHNOLOGY LABORATORY
AVRADCOM
ATTN DAVDL-ATL-TSD, TECH LIBRARY
FT EUSTIS, VA 23604

COMMANDER
US ARMY ARMAMENT RESEARCH &
DEVELOPMENT COMMAND
ATTN DRDAR-FU, PROJECT MGT PROJECT OFC
ATTN DRCPM-CAWS, PM, CANNON ARTILLERY
WEAPONS SYSTEMS/SEMI-ACTIVE
LASER GUIDED PROJECTILES
ATTN DRCPM-SA, PM, SELECTED AMMUNITION
ATTN DRDAR-TDR, RESEARCH & TECHNOLOGY
ATTN DRDAR-TDS, SYSTEMS DEV &
ENGINEERING
ATTN DRDAR-SE, SYSTEMS EVALUATION
OFFICE
ATTN DRDAR-PM, PROGRAM MANAGEMENT
SUPPORT OFFICE
ATTN DRDAR-LC, LARGE CALIBER WEAPON
SYSTEMS LABORATORY
ATTN DRDAR-SC, FIRE CONTROL & SMALL
CALIBER WEAPON SYSTEMS LABORATORY
ATTN DRDAR-TS, TECHNICAL SUPPORT DIV
ATTN DRDAR-QA, PRODUCT ASSURANCE DIV
DOVER, NJ 07801

COMMANDER/DIRECTOR
ATMOSPHERIC SCIENCES LABORATORY
US ARMY ERADCOM
ATTN DELAS-AS, ATMOSPHERIC SENSING DIV
ATTN DELAS-AS-T, TACTICAL SENSOR BR
ATTN DELAS-BE, BATTLEFIELD ENVIR DIV
ATTN DELAS-BR, ATMOSPHERIC EFFECTS BR
ATTN DELAS-BE-C, COMBAT ENVIR BR
ATTN DELAS-EO, ELECTRO/OPTICS DIVISION
WHITE SANDS MISSILE RANGE, NM 88002

PRESIDENT
US ARMY AVIATION BOARD
ATTN ATZQ-OT-CO, TEST CONCEPT &
OPERATIONS DIV
ATTN ATZQ-OT-CM, CONCEPT &
METHODOLOGY BR
ATTN ATZQ-OT-ES, ELECTRONIC SYS TEST
BRANCH
FT RUCKER, AL 36360

COMMANDER
US ARMY AVIONICS RES & DEV ACTIVITY
ATTN DAVAA-I AVIATION ELECTRONICS
INTEGRATION DIV
ATTN DAVAA-E, COMMUNICATIONS & SENSOR
DIV
FT MONMOUTH, NJ 07703

COMMANDER
US ARMY AVIATION RESEARCH &
DEVELOPMENT COMMAND
ATTN DRDAV-N, DIR FOR ADVANCED SYSTEMS
ATTN DRDAV-E, DIR FOR SYSTEMS
ENGINEERING & DEVELOPMENT
PO BOX 209
ST LOUIS, MO 63166

PRESIDENT
US ARMY ARMOR & ENGINEER BOARD
ATTN ATZK-AE-IN-O, OPTICAL
INSTRUMENTATION BRANCH
ATTN ATZK-AE-IN-E, ELECTRONIC
INSTRUMENTATION BRANCH
ATTN ATZK-AE-TA, TEST DESIGN &
ANALYSIS DIV
ATTN ATZK-AE-CV, COMBAT VEHICLE
TECHNOLOGY DIR
FT KNOX, KY 40121

BALLISTIC MISSILE DEFENSE PROGRAM
MANAGER OFFICE
ATTN DACS-BMZ-C, DEPUTY DIR
5001 EISENHOWER AVE
ALEXANDRIA, VA 22333

COMMANDER
BALLISTIC MISSILE DEFENSE
SYSTEMS COMMAND
PO BOX 1500
HUNTSVILLE, AL 35807

DIRECTOR
BMD ADVANCED TECHNOLOGY CENTER
DEPARTMENT OF THE ARMY
PO BOX 1500
ATTN ATC-T
ATTN ATC-D
HUNTSVILLE, AL 35807

DIRECTOR
US ARMY BALLISTIC RESEARCH LABORATORY
ATTN DRDAR-BLV, VULNERABILITY/
LETHALITY DIV
ATTN DRDAR-BLB, BALLISTICS MODELING DIV
ATTN DRDAR-BLP, PROPULSION DIV
ATTN DRDAR-BLL, LAUNCH & FLIGHT DIV
ATTN DRDAR-BLT, TERMINAL BALLISTICS DIV
ABERDEEN PROVING GROUND, MD 21005

COMMANDER
USARRADCOM
BENET WEAPONS LAB LCWSL
WATERVLIET, NY 12189

COMMANDER/DIRECTOR
CHEMICAL SYSTEMS LABORATORY
ARRADCOM
ATTN DRDAR-CLJ-L, TECHNICAL LIBRARY BR
ABERDEEN PROVING GROUND, MD 21010

COMMANDER
US ARMY COLD REGIONS
RESEARCH & ENGINEERING LABORATORY
ATTN CRREL-CS, CHIEF SCIENTIST
ATTN CRREL-RD, RESEARCH DIVISION
ATTN CRREL-EE, EXPERIMENTAL
ENGINEERING DIV
ATTN CRREL-TI, TECHNICAL INFO BR
HANOVER, NH 03755

COMMANDER/DIRECTOR
COMBAT SURVEILLANCE
& TARGET ACQUISITION LABORATORY
US ARMY ERADCOM
ATTN DELCS-DT, CHIEF TECHNICAL PLANS &
MGT OFFICE
ATTN DELCS-R, DIR RADAR DIV
ATTN DELCS-X, DIR DATA XMSM &
SYS DIV
ATTN DELCS-S, DIR SPECIAL SENSORS DIV
ATTN DELCS-PA, DIR PRODUCT ASSURANCE &
TEST OFFICE
FT MONMOUTH, NJ 07703

COMMANDER
COMBAT DEVELOPMENTS
EXPERIMENTATION COMMAND
FT ORD, CA 93941

COMMANDER
US ARMY COMBINED ARMS COMBAT
DEVELOPMENTS ACTIVITY
FT LEAVENWORTH, KS 66027

DIRECTORATE OF COMBAT
DEVELOPMENTS
US ARMY ARMOR CENTER
FT KNOX, KY 40121

CHIEF
US ARMY COMMUNICATIONS SYS AGENCY
FT MONMOUTH, NJ 07703

COMMANDER
US ARMY COMMUNICATIONS & ELECTRONICS
MATERIEL READINESS COMMAND
FT MONMOUTH, NJ 07703

COMMANDER
US ARMY COMM-ELEC ENGR INSTAL AGENCY
ATTN TECH LIB
FT HUACHUCA, AZ 85613

COMMANDER
US ARMY COMMUNICATIONS COMMAND
COMBAT DEVELOPMENT DIV
FT HUACHUCA, AZ 85613

COMMANDER
US ARMY COMMUNICATIONS RESEARCH &
DEVELOPMENT COMMAND
ATTN DRCPM-TF, OFC OF THE PM TACTICAL
FIRE DIRECTION SYS/FIELD ARTILLERY
TACTICAL DATA SYSTEMS
(TACFIRE/FATDS)
ATTN DRCPM-MSCS, OFC OF THE PM MULTI-
SERVICE COMMUNICATIONS SYS
ATTN DRCPM-ATC, OFC OF THE PM ARMY
TACTICAL COMMUNICATIONS
SYS (ATACS)
ATTN DRDCO-PPA, PLANS, PROGRAMS &
ANALYSIS DIR
ATTN DRDCO-TCS, CENTER FOR TACTICAL
COMPUTER SYS
ATTN DRDCO-COM, CENTER FOR
COMMUNICATIONS SYS
ATTN DRDCO-SEI, SYS ENGINEERING
& INTEGRATION (CENSEI)
FT MONMOUTH, NJ 07703

COMMANDER
US ARMY COMMUNICATIONS COMMAND
USA COMMO AGENCY, WS
WHITE SANDS MISSILE RANGE, NM 88002

COMMANDER
US ARMY COMPUTER SYSTEMS COMMAND
ATTN TECH LIB
FT BELVOIR, VA 22060

DEPARTMENT OF THE ARMY
CONCEPT ANALYSIS AGENCY
8120 WOODMONT AVE
BETHESDA, MD 20014

DIRECTOR
CONSTRUCTION ENGINEERING RSCH LAB
DEPARTMENT OF THE ARMY
PO BOX 4005
CHAMPAIGN, IL 61820

COMMANDER
ERADCOM TECHNICAL SUPPORT ACTIVITY
ATTN DELSD-L, TECH LIB DIR
FT MONMOUTH, NJ 07703

DIRECTOR
ELECTRONICS TECHNOLOGY &
DEVICES LABORATORY
US ARMY ERADCOM
ATTN DELET-DT, DIR TECHNICAL PLANS &
PROGRAMS OFFICE
ATTN DELET-E, DIR ELECTRONIC MATERIALS
RESEARCH DIV
ATTN DELET-I, DIR MICROELECTRONICS DIV
ATTN DELET-M, MICROWAVE & SIGNAL
PROCESSING DEVICES DIV
FT MONMOUTH, NJ 07703

DIRECTOR
ELECTRONIC WARFARE LABORATORY
ATTN DELEW-SM, EW SYSTEMS MGT OFFICE
ATTN DELEW-C, COMM INTEL/CM DIV
ATTN DELEW-E, ELCT INTEL/CM DIV
ATTN DELEW-V, EM VULN & ECCM DIV
FT MONMOUTH, NJ 07703

DIRECTOR
US ARMY ENGINEER WATERWAYS
EXPERIMENT STATION
PO BOX 631
ATTN TECHNICAL INFORMATION CENTER
VICKSBURG, MS 39180

PRESIDENT
US ARMY FIELD ARTILLERY BOARD
ATTN ATZR-BDWT, WEAPONS TEST DIV
ATTN ATZR-BDAS, ARTILLERY SPT TEST DIV
FT SILL, OK 73503

COMMANDING OFFICER
US ARMY FOREIGN SCIENCE
& TECHNOLOGY CENTER
FEDERAL OFFICE BLDG
220 7TH STREET, NE
ATTN DRXST-SC, SCIENCES DIV
ATTN DRXST-ES, ELECTRONICS SYS DIV
ATTN DRCST-SD-1, C. WARD
CHARLOTTESVILLE, VA 22901

COMMANDER
EWL
INTEL MAT DEV & SPT OFFICE
ATTN DELEW-I
FT MEADE, MD 20755

DIRECTOR
US ARMY HUMAN ENGINEERING LABORATORY
ATTN DRXHE-BR, BEHAVIORAL RESEARCH DIV
ATTN DRXHE-TS, TECHNICAL SUPPORT DIV
ATTN DRXHE-HE, HUMAN ENGINEERING
APPLICATIONS DIR

US ARMY HUMAN ENGINEERING LABORATORY
(Cont'd)
ATTN DRXHE-SP, SYSTEMS PERFORMANCE
& CONCEPTS DIR
ATTN DRXHE-PC, TECH LIBRARY
ABERDEEN PROVING GROUND, MD 21005

PRESIDENT
US ARMY INFANTRY BOARD
ATTN ATZB-IB-TS, TEST SUPPORT DIV
ATTN ATZB-IB-TS-A, ANALYSIS &
EVALUATION BR
ATTN ATZB-IB-TS-D, RANGE CONTROL &
DATA ACQUISITION BR
ATTN ATZB-IB-AT, ANTIARMOR TEST DIV
ATTN ATZB-IB-SA, SMALL ARMS TEST DIV
FT BENNING, GA 31905

COMMANDER
US ARMY INTELLIGENCE & SEC COMMAND
ATTN TECH LIBRARY
ARLINGTON HALL STATION
4000 ARLINGTON BLVD
ARLINGTON, VA 22212

PRESIDENT/COMMANDER
US ARMY INTELLIGENCE &
SECURITY BOARD
ATTN ATSI-BD-EW, ELECTRONIC WARFARE
TESTS
ATTN STEEP-MT-EW, INTEL &
COMMUNICATIONS BR
ATTN STEEP-MT-EW, COMMUNICATIONS
SYS SECT
ATTN STEEP-MT-EW, NON-COMMUNICATIONS
SYS SECT
FT HUACHUCA, AZ 85613

COMMANDER
US ARMY MATERIEL DEVELOPMENT
& READINESS COMMAND
ATTN DRCPA, DIR FOR PLANS &
ANALYSIS
ATTN DRCNC, NUCLEAR-CHEMICAL OFFICE
ATTN DRCDE, DIR FOR DEVELOPMENT & ENG
ATTN DRCPM, OFFICE OF PROJECT
MANAGEMENT
5001 EISENHOWER AVE
ALEXANDRIA, VA 22333

COMMANDER
US ARMY MATERIEL SYSTEMS ANALYSIS
ACTIVITY
ATTN X5 (W3JCAA)
ABERDEEN PROVING GROUND, MD 21005

COMMANDER
US ARMY MATERIALS & MECHANICS
RESEARCH CENTER
ATTN DRXMR-PL, TECHNICAL LIBRARY

US ARMY MATERIALS & MECHANICS
RESEARCH CENTER (Cont'd)
ATTN DRXMR-T, MECHANICS & ENGINEERING
LABORATORY
ATTN DRXMR-M, MATERIALS TESTING
TECHNOLOGY DIV
ATTN DRXMR-R, ORGANIC MATERIALS
LABORATORY
ATTN DRXMR-E, METALS & CERAMICS
LABORATORY
WATERTOWN, MA 02172

COMMANDER
US ARMY MISSILE COMMAND
ATTN DRCPM-CF, CHAPARRAL/FAAR
ATTN DRCPM-HD, HELLFIRE/GLD
ATTN DRCPM-PE, PERSHING
ATTN DRCPM-DT, TOW DRAGON
ATTN DRCPM-RS, GENERAL SUPPORT
ROCKET SYS
ATTN DRCPM-HEL, HIGH ENERGY LASER SYS
ATTN DRCPM-ROL, ROLAND
ATTN DRCPM-VI, VIPER
ATTN DRCPM-HA, HAWK
ATTN DRCPM-LC, LANCE
ATTN DRCPM-MP, STINGER
ATTN DRSMI-O, ADVANCED SYS CONCEPTS
OFFICE
ATTN DRSMI-V, COPPERHEAD
ATTN DRSMI-T, TARGETS MANAGEMENT OFFICE
ATTN DRSMI-U, WEAPONS SYS MGT DIR
ATTN DRSMI-D, PLANS, ANALYSIS,
& EVALUATION
ATTN DRSMI-E, ENGINEERING
ATTN DRSMI-Q, PRODUCT ASSURANCE
ATTN DRSMI-S, MATERIEL MANAGEMENT
ATTN DRSMI-W, MGMT INFO SYSTEMS
REDSTONE ARSENAL, AL 35809

DIRECTOR
US ARMY MISSILE LABORATORY
USAMICOM
ATTN DRSMI-RPR, REDSTONE SCIENTIFIC
INFO CENTER
ATTN DRSMI-RPT, TECHNICAL
INFORMATION DIV
ATTN DRSMI-RN, CHIEF, TECHNOLOGY
INTEGRATION OFFICE
ATTN DRSMI-RA, CHIEF, DARPA PROJECTS
OFFICE
ATTN DRSMI-RH, DIR, DIRECTED ENERGY
DIRECTORATE
ATTN DRSMI-RL, SPE ASST GROUND EQUIP &
MISSILE STRUCTURES DIR
ATTN DRSMI-RR, RESEARCH DIR
ATTN DRSMI-RS, SYS ENGR DIR
ATTN DRSMI-RT, TEST & EVAL DIR
ATTN DRSMI-RD, SYS SIMULATION & DEV DIR
ATTN DRSMI-RE, ADVANCED SENSORS DIR
ATTN DRSMI-RK, PROPULSION DIR
ATTN DRSMI-RG, GUIDANCE & CONTROL DIR
REDSTONE ARSENAL, AL 35809

COMMANDER & DIRECTOR
OFC OF MISSILE ELCT WARFARE
ATTN DELEW-M-PM, PROG MGT SPT OFFICE
ATTN DELEW-M-ST, SURFACE TARGET DIV
ATTN DELEW-M-TA, TECH & ADV
CONCEPTS DIV
WHITE SANDS MISSILE RANGE, NM 88002

COMMANDER
US ARMY MOBILITY EQUIPMENT
RESEARCH & DEVELOPMENT COMMAND
ATTN DRDME-U, PROGRAMS & ANALYSIS DIR
ATTN DRDME-T, PRODUCT ASSURANCE &
TESTING DIR
ATTN DRDME-V, MATERIAL TECHNOLOGY
LABORATORY
FT BELVOIR, VA 22060

COMMANDER
US ARMY NATICK RES & DEV COMMAND
NATICK DEVELOPMENT CENTER
ATTN DRDNA-T, TECHNICAL LIBRARY
ATTN DRDNA-E, CHIEF ENGINEERING
PROGRAMS MANAGEMENT OFFICE
ATTN DRDNA-U, DIR AERO-MECHANICAL
ENGINEERING LABORATORY
ATTN DRDNA-O, CHIEF OPERATIONS RESEARCH
SYSTEMS ANALYSIS OFFICE
NATICK, MA 01760

DIRECTOR
NIGHT VISION & ELECTRO-OPTICS
LABORATORY
ATTN DELNV-D, AD FOR DEV & ENGRG
ATTN DELNV-PA, PRODUCT ASSURANCE DIV
ATTN DELNV-AC, ADVANCED CONCEPTS DIV
ATTN DELNV-AC, TARGET ACQUISITION RES
ATTN DELNV-IRT, INFRARED TECHNOLOGY DIV
ATTN DELNV-L, LASER DIVISION
ATTN DELNV-R, ELECTRO-OPTICS RES
ATTN DELNV-R, ELECTRONICS MATERIALS RES
ATTN DELNV-SE, SYSTEMS ENGINEERING DIV
ATTN DELNV-SE, MISSILES
ATTN DELNV-SI, SYSTEMS INTEGRATION DIV
ATTN DELNV-SI, COMBAT VEHICLES
ATTN DELNV-SI, OPTICS
ATTN DELNV-SI, ELECTRONICS
ATTN DELNV-VI, VISIONIC DIVISION
ATTN DELNV-VI, BATTLEFIELD ENVIRONMENT
ATTN DELNV-VI, BATTLEFIELD SYSTEMS
PERFORMANCE
FT BELVOIR, VA 22060

COMMANDER
US ARMY NUCLEAR & CHEMICAL AGENCY
ATTN ATCN-W, WEAPONS EFFECTS DIV
7500 BACKLICK ROAD
BUILDING 2073
SPRINGFIELD, VA 22150

COMMANDER
US ARMY OPERATIONAL TEST
& EVALUATION AGENCY
5600 COLUMBIA PIKE
FALLS CHURCH, VA 22041

DIRECTOR
PROPULSION LABORATORY
RESEARCH & TECHNOLOGY LABORATORIES
AVRADCOM
LEWIS RESEARCH CENTER, MS. 106-2
21000 BROOKPARK ROAD
CLEVELAND, OH 44135

DIRECTOR
US ARMY RESEARCH & TECHNOLOGY
LABORATORIES
AMES RESEARCH CENTER
MOFFETT FIELD, CA 94035

US CHIEF ARMY RESEARCH OFFICE (DURHAM)
PO BOX 12211
ATTN DRXRO-EL, DIR ELECTRONICS DIV
ATTN DRXRO-MA, DIR MATHEMATICS DIV
ATTN DRXRO-CB, DIR CHEMICAL-BIOLOGICAL
DIV
ATTN DRXRO-PH, DIR PHYSICS DIV
ATTN DRXRO-MS, METALLURGY-MATERIALS
DIV
ATTN DRXRO-EG, DIR ENGINEERING DIV
RESEARCH TRIANGLE PARK, NC 27709

DIRECTOR
RESEARCH & TECHNOLOGY
LABORATORIES (AVRADCOM)
AMES RESEARCH CENTER
MOFFETT FIELD, CA 94035

OFFICE OF THE DEPUTY CHIEF OF STAFF
FOR RESEARCH, DEVELOPMENT,
& ACQUISITION
ATTN DIR OF ARMY RES, DAMA-ARZ-A
DR. M. E. LASSER
ATTN DAMA-RAX, SYSTEMS REVIEW &
ANALYSIS OFFICE
ATTN DAMA-ZE, ADVANCED CONCEPTS TEAM
ATTN DAMD-CSZ-A, DIR OF COMBAT
SUPPORT SYSTEMS
ATTN DAMA-WSZ-A, DIR OF WEAPONS SYSTEMS
ATTN DAMA-PPZ-A, DIR OF MATERIAL PLANS
& PROGRAMS
ATTN DAMA-CSC, COMMAND, CONTROL,
SURVEILLANCE SYSTEMS DIV
ATTN DAMA-WSA, AVIATION SYSTEMS DIV
ATTN DAMA-CSM, MUNITIONS DIV
ATTN DAMA-WSM, MISSILES & AIR
DEFENSE SYSTEMS DIV
ATTN DAMA-CSS, SUPPORT SYSTEMS DIV
ATTN DAMA-WSW, GROUND COMBAT
SYSTEMS DIV
WASHINGTON, DC 20310

US ARMY SATELLITE COMMUNICATIONS
AGENCY
CORADCOM
FT MONMOUTH, NJ 07703

COMMANDER
US ARMY SATELLITE COMM
AGENCY
FT MONMOUTH, NJ 07703

COMMANDER
US ARMY SIGNAL CENTER
& FT GORDON
ATTN ATZHTD, DIR OF COMBAT
DEVELOPMENTS
ATTN ATZHTD-A-C, CTAD BRANCH
ATTN ATZHTD-A-DA, C-E DATA/
AVIONICS BRANCH
ATTN ATZHTD-A-M, C-E MAINTENANCE
BRANCH
ATTN ATZHTD-A-AV, C-E MANAGEMENT/
AUDIO-VISUAL BRANCH
ATTN ATZHTD-D, DOCTRINE BRANCH
ATTN ATZHTD-D, DESIGN & DEVELOPMENT
DIV
ATTN ATZHCE, DIR OF COMMUNICATIONS
AND ELECTRONICS
FT GORDON, GA 30905

DIRECTOR
US ARMY SIGNALS WARFARE LABORATORY
VINT HILL FARMS STATION
ATTN DELSW-RA, ANALYSIS &
APPLICATIONS DIV
ATTN DELSW-CE, COMMUNICATIONS/EW
DIVISION
ATTN DELSW-EE, ELECTRONICS/EW DIVISION
ATTN DELSW-GD, GENERAL SUPPORT SYSTEMS
DIVISION
ATTN DELSW-OS, OFFICE OF THE SCIENTIFIC
ADVISOR
ATTN DELSW-CAC, PROJECT MANAGER--
CONTROL & ANALYSIS CENTERS OFFICE
ATTN DELSW-M, RESOURCE MANAGEMENT &
PLANS DIVISION
ATTN DELSW-SS, SIGNAL SECURITY OFFICE
ATTN DELSW-DT, TACTICAL DATA SYSTEMS
DIVISION
WARRENTON, VA 22186

COMMANDER
US ARMY TANK-AUTOMOTIVE COMMAND
ATTN DRCPM-CVT, ARMORED COMBAT
VEHICLE TECHNOLOGY
ATTN DRCPM-ITV, IMPROVED TOW VEHICLE
ATTN DRDTR-R, TANK-AUTOMOTIVE SYSTEMS
LABORATORY
ATTN DRDTR-Z, TANK-AUTOMOTIVE CONCEPTS
LABORATORY

DISTRIBUTION (Cont'd)

US ARMY TANK-AUTOMOTIVE COMMAND
ATTN DRDTR-T, DIR FOR ENGINEERING
SUPPORT
ATTN DRDTR-J, DIR FOR PRODUCT ASSURANCE
28251 VAN DYKE AVE
WARREN, MI 48090

COMMANDER
US ARMY TEST & EVALUATION
COMMAND
ABERDEEN PROVING GROUND, MD 21005

COMMANDER
US ARMY TRAINING & DOCTRINE
COMMAND
ATTN ATCD-DCS, COMBAT DEVELOPMENT
ATTN ATCD-AN, ANALYSIS DIR
ATTN ATCD-AN, COMBAT SYS BR
ATTN ATCD-AN, METHODOLOGY BR
ATTN ATCD-C, TELECOM COMD & CON &
COMPTR SYS DIR
ATTN ATCD-C, BATTLEFIELD SYS
INTEGRATION BR
ATTN ATCD-IE, INTEL & EW DIR
ATTN ATCD-IE, ELECTRONIC WARFARE BR
ATTN ATCD-T, TEST & EVAL DIR
ATTN DCS COMBAT DEVELOPMENTS--ATCD
ATTN DCS TRAINING-ATTNG
ATTN INFO OFFICE--ATID
ATTN COMM & ELECTRONICS--ATCE
FT MONROE, VA 23651

COMMANDER
US ARMY TRAINING & DOCTRINE
COMMAND SYS ANALYSIS ACTIVITY
WHITE SANDS MISSILE RANGE, NM 88002

COMMANDER
WHITE SANDS MISSILE RANGE
DEPT OF THE ARMY
ATTN STEWS-CE, COMMUNICATIONS/
ELEC OFFICE
WHITE SANDS MISSILE RANGE, NM 88002

COMMANDER
EDGEWOOD ARSENAL
ABERDEEN PROVING GROUND, MD 21005

COMMANDER
WATERVLIET ARSENAL
WATERVLIET, NY 12189

COMMANDER
US ARMY ABERDEEN PROVING GROUND
ATTN STEAP-TL, TECH LIB
ABERDEEN PROVING GROUND, MD 21005

COMMANDER
US ARMY DUGWAY PROVING GROUND
DUGWAY, UT 84022

COMMANDER
US ARMY ELECTRONICS PROVING GROUND
FT HUACHUCA, AZ 85613

COMMANDER
US ARMY YUMA PROVING GROUND
YUMA, AZ 85364

COMMANDANT
US ARMY FIELD ARTILLERY SCHOOL
ATTN LIBRARY
FT SILL, OK 73503

COMMANDANT
US ARMY ENGINEER SCHOOL
ATTN LIBRARY
FT BELVOIR, VA 22060

COMMANDANT
US ARMY INFANTRY SCHOOL
ATTN LIBRARY
FT BENNING, GA 31905

COMMANDANT
US ARMY WAR COLLEGE
ATTN LIBRARY
CARLISLE BARRACKS, PA 17013

COMMANDER
US ARMY ORDNANCE
CENTER & SCHOOL
ABERDEEN PROVING GROUND, MD 21005

ASSISTANT SECRETARY OF THE NAVY
RESEARCH, ENGINEERING, & SYSTEMS
DEPT OF THE NAVY
WASHINGTON, DC 20350

COMMANDER
NAVAL AIR DEVELOPMENT CENTER
ATTN TECHNICAL LIBRARY
WARMINSTER, PA 18974

COMMANDER
NAVAL AIR SYSTEMS COMMAND HQ
DEPT OF THE NAVY
WASHINGTON, DC 20361

OFFICER-IN-CHARGE
NAVAL CONSTRUCTION BATTALION CENTER
CIVIL ENGINEERING LABORATORY
ATTN CODE L51
PORT HUENEME, CA 93041

HQ NAVAL MATERIAL COMMAND
DEPT OF THE NAVY
WASHINGTON, DC 20360

CHIEF OF NAVAL OPERATIONS
DEPT OF THE NAVY
ATTN DIR, COM & CONTR &
COMMUNICATIONS PROGRAMS
WASHINGTON, DC 20350

COMMANDER
NAVAL OCEAN SYSTEMS CENTER
SAN DIEGO, CA 92152

SUPERINTENDENT
NAVAL POSTGRADUATE SCHOOL
ATTN LIBRARY, CODE 2124
MONTEREY, CA 93940

DIRECTOR
NAVAL RESEARCH LABORATORY
ATTN 2600, TECHNICAL INFO DIV
ATTN 2750, OPTICAL SCIENCES DIV
ATTN 5500, OPTICAL SCI DIV
ATTN 6000, MATL & RADIATION
SCI & TE
WASHINGTON, DC 20375

CHIEF OF NAVAL RESEARCH
DEPT OF THE NAVY
ATTN ONR-400, ASST CH FOR RES
ATTN ONR-420, PHYSICAL SCI DIV
ARLINGTON, VA 22217

COMMANDER
NAVAL SHIP ENGINEERING CENTER
WASHINGTON, DC 20360

COMMANDER
DAVID W. TAYLOR NAVAL SHIP R&D CENTER
BETHESDA, MD 20084

COMMANDER
NAVAL SURFACE WEAPONS CENTER
ATTN DX-21 LIBRARY DIV
DAHLGREN, VA 22448

COMMANDER
NAVAL SURFACE WEAPONS CENTER
ATTN F30, NUCLEAR EFFECTS DIV
ATTN R-40, RADIATION DIV
ATTN R-42, ELECTRO-OPTICS BR
ATTN E-40, TECHNICAL LIB
WHITE OAK, MD 20910

COMMANDER
NAVAL TELECOMMUNICATIONS COMMAND HQ
ATTN TECHNICAL LIBRARY
4401 MASS AVE NW
WASHINGTON, DC 20390

COMMANDER
NAVAL WEAPONS CENTER
ATTN 38, RESEARCH DEPT
ATTN 381, PHYSICS DIV
CHINA LAKE, CA 93555

COMMANDING OFFICER
NAVAL WEAPONS EVALUATION FACILITY
KIRTLAND AIR FORCE BASE
ALBUQUERQUE, NM 87117

DEPUTY CHIEF OF STAFF
RESEARCH & DEVELOPMENT
HEADQUARTERS, US AIR FORCE
ATTN AFRDQSM
WASHINGTON, DC 20330

SUPERINTENDENT
HQ US AIR FORCE ACADEMY
ATTN TECH LIB
USAF ACADEMY, CO 80840

AF AERO-PROPULSION LABORATORY
WRIGHT-PATTERSON AFB, OH 45433

COMMANDER
ARNOLD ENGINEERING DEVELOPMENT CENTER
ATTN DY, DIR TECHNOLOGY
ARNOLD AIR FORCE STATION, TN 37389

AIR FORCE AVIONICS LABORATORY
ATTN KJA (TEO), ELECTRO-OPTICS
TECHNOLOGY BR
WRIGHT-PATTERSON AFB, OH 45433

COMMANDER
HQ AF DATA AUTOMATION AGENCY
ATTN DATA SYS EVAL OFFICE
GUNTER AFS, AL 36114

COMMANDER
AF ELECTRONIC SYSTEMS DIVISION
ATTN WO, DEP FOR CONTROL
& COMMUNICATIONS SYS
L. G. HANSCOM AFB, MA 01730

RELIABILITY ANALYSIS CENTER
RADC (RBRAC)
GRIFFISS AFB, NY 13441

COMMANDER
HQ ROME AIR DEVELOPMENT CENTER (AFSC)
ATTN LE, DEPUTY FOR ELECTRONIC TECH
ATTN LMT, TELECOMMUNICATIONS BR
GRIFFISS AFB, NY 13441

SAMSO/CC
PO BOX 92960
WORLDWAY POSTAL CENTER
LOS ANGELES, CA 90009

DISTRIBUTION (Cont'd)

DIRECTOR
AF OFFICE OF SCIENTIFIC RESEARCH
BOLLING AFB
ATTN NE, DIR OF ELECTRONIC &
SOLID STATE SCI
WASHINGTON, DC 20332

COMMANDER
HQ AIR FORCE SYSTEMS COMMAND
ANDREWS AFB
ATTN TECHNICAL LIBRARY
WASHINGTON, DC 20334

AF WEAPONS LABORATORY, AFSC
ATTN EL, ELECTRONICS DIV
ATTN LR, LASER DEV DIV
KIRTLAND AFB, NM 87117

AMES RESEARCH CENTER
NASA
ATTN TECHNICAL INFO DIV
MOFFETT FIELD, CA 94035

DIRECTOR
NASA
GODDARD SPACE FLIGHT CENTER
ATTN 250, TECH INFO DIV
GREENBELT, MD 20771

DIRECTOR
NASA
ATTN TECHNICAL LIBRARY
JOHN F. KENNEDY SPACE
CENTER, FL 32899

DIRECTOR
NASA
LANGLEY RESEARCH CENTER
ATTN TECHNICAL LIBRARY
HAMPTON, VA 23665

DIRECTOR
NASA
LEWIS RESEARCH CENTER
ATTN TECHNICAL LIBRARY
CLEVELAND, OH 44135

JET PROPULSION LABORATORY
CALIFORNIA INSTITUTE OF TECHNOLOGY
4800 OAK GROVE DRIVE
ATTN TECHNICAL LIBRARY
PASADENA, CA 91103

LAWRENCE LIVERMORE NATIONAL LABORATORY
PO BOX 808
LIVERMORE, CA 94550

CATHOLIC UNIVERSITY OF AMERICA
CARDINAL STATION
PO BOX 232
WASHINGTON, DC 20017

UNIVERSITY OF CALIFORNIA
SCHOOL OF ENGINEERING
LOS ANGELES, CA 90024

RUTGERS UNIVERSITY
COLLEGE OF ENGINEERING
DEPARTMENT OF CERAMICS
NEW BRUNSWICK, NJ 08903

SANDIA LABORATORIES
LIVERMORE LABORATORY
PO BOX 969
LIVERMORE, CA 94550

SANDIA NATIONAL LABORATORIES
PO BOX 5800
ALBUQUERQUE, NM 87185

CIVIL ENGINEERING RESEARCH FACILITY
UNIVERSITY OF NEW MEXICO
PO BOX 188
ALBUQUERQUE, NM 87131

US ARMY ELECTRONICS RESEARCH
& DEVELOPMENT COMMAND
ATTN TECHNICAL DIRECTOR, DRDEL-CT

HARRY DIAMOND LABORATORIES
ATTN CO/TD/TSO/DIVISION DIRECTORS
ATTN RECORD COPY, 81200
ATTN HDL LIBRARY, 81100 (2 COPIES)
ATTN HDL LIBRARY, 81100 (WOODBRIDGE)
ATTN TECHNICAL REPORTS BRANCH, 81300
ATTN LEGAL OFFICE, 97000
ATTN CHAIRMAN, EDITORIAL COMMITTEE
ATTN MORRISON, R. E., 13500 (GIDEP)
ATTN CHIEF, 21000
ATTN CHIEF, 21100
ATTN CHIEF, 21200
ATTN CHIEF, 21300
ATTN CHIEF, 21400
ATTN CHIEF, 21500
ATTN CHIEF, 22000
ATTN CHIEF, 22100
ATTN CHIEF, 22300
ATTN CHIEF, 22800
ATTN CHIEF, 22900
ATTN CHIEF, 20240
ATTN BRANDT, H. E., 22300
ATTN SOLN, J., 22300
ATTN MEYER, O. L., 22800
ATTN WHITTAKER, D. A., 22900
ATTN MERKLE, G., 21300 (5 COPIES)